TECHNISCHE UNIVERSITÄT WIEN
Vienna University of Technology

AUTOMATION & CONTROL INSTITUTE
INSTITUT FÜR AUTOMATISIERUNGS- & REGELUNGSTECHNIK

This document contains a post-print version of the paper

A mathematical model of a slab reheating furnace with radiative heat transfer and non-participating gaseous media

authored by **A. Steinboeck, D. Wild, T. Kiefer, and A. Kugi**

and published in *International Journal of Heat and Mass Transfer.*

The content of this post-print version is identical to the published paper but without the publisher's final layout or copy editing. Please, scroll down for the article.

Cite this article as:

A. Steinboeck, D. Wild, T. Kiefer, and A. Kugi, "A mathematical model of a slab reheating furnace with radiative heat transfer and non-participating gaseous media", *International Journal of Heat and Mass Transfer*, vol. 53, no. 25-26, pp. 5933–5946, 2010. DOI: 10.1016/j.ijheatmasstransfer.2010.07.029

BibTex entry:

```
@ARTICLE{steinboeck10a,
  AUTHOR = {Steinboeck, A. and Wild, D. and Kiefer, T. and Kugi, A.},
  TITLE = {A mathematical model of a slab reheating furnace with radiative heat transfer and non-
      participating gaseous media},
  JOURNAL = {International Journal of Heat and Mass Transfer},
  YEAR = {2010},
  volume = {53},
  number = {25-26},
  pages = {5933-5946},
  doi = {10.1016/j.ijheatmasstransfer.2010.07.029},
  url = {http://www.sciencedirect.com/science/article/pii/S0017931010003996}
}
```

Link to original paper:

http://dx.doi.org/10.1016/j.ijheatmasstransfer.2010.07.029
http://www.sciencedirect.com/science/article/pii/S0017931010003996

Read more ACIN papers or get this document:

http://www.acin.tuwien.ac.at/literature

Contact:

Automation and Control Institute (ACIN)
Vienna University of Technology
Gusshausstrasse 27-29/E376
1040 Vienna, Austria

Internet: www.acin.tuwien.ac.at
E-mail: office@acin.tuwien.ac.at
Phone: +43 1 58801 37601
Fax: +43 1 58801 37699

Copyright notice:

This is the authors' version of a work that was accepted for publication in International Journal of Heat and Mass Transfer. Changes resulting from the publishing process, such as peer review, editing, corrections, structural formatting, and other quality control mechanisms may not be reflected in this document. Changes may have been made to this work since it was submitted for publication. A definitive version was subsequently published in A. Steinboeck, D. Wild, T. Kiefer, and A. Kugi, "A mathematical model of a slab reheating furnace with radiative heat transfer and non-participating gaseous media", *International Journal of Heat and Mass Transfer*, vol. 53, no. 25-26, pp. 5933–5946, 2010. DOI: 10.1016/j.ijheatmasstransfer.2010.07.029

A mathematical model of a slab reheating furnace with radiative heat transfer and non-participating gaseous media

A. Steinboeck*[,a], D. Wild[b], T. Kiefer[b], A. Kugi[a]

[a] *Automation and Control Institute, Vienna University of Technology, Gusshausstrasse 27–29, 1040 Wien, Austria*
[b] *AG der Dillinger Hüttenwerke, Werkstrasse 1, 66763 Dillingen/Saar, Germany*

Abstract

A mathematical model of the reheating process of steel slabs in industrial fuel-fired furnaces is developed. The transient temperature field inside the slabs is computed by means of the Galerkin method. Radiative heat transfer inside the furnace constitutes boundary conditions that couple the dynamic subsystems of the slabs. Constraining the heat fluxes to piecewise linear, discontinuous signals furnishes a discrete-time state-space system. Conditions for an exponential decrease of the open-loop control error are derived. Measurements from an instrumented slab in the real system demonstrate the accuracy of the model. The simple and computationally inexpensive model is suitable for trajectory planning, optimization, and controller design.

Key words: Reheating furnace, steel slab reheating, transient heat conduction, Galerkin method, radiative heat exchange, open-loop control

Nomenclature

$\mathbf{1}$	vector of unity components (−)
$\boldsymbol{A}$, $\boldsymbol{a}_j$	dynamic matrices (1/s)
$\tilde{\boldsymbol{a}}_j$	transformed dynamic matrix (1/s)
a	bilinear form
$\mathcal{B}_j^{\mp}$	differential operator of boundary condition ($\mathrm{W/m^2}$)
$\boldsymbol{B}$	vector of radiosities ($\mathrm{W/m^2}$)
$\boldsymbol{B}^{\mp}$	input gain matrix ($\mathrm{K\,m^2/J}$)
$\boldsymbol{b}_j$	input gain vector ($\mathrm{K\,m^2/J}$)
$\tilde{\boldsymbol{b}}_j$	transformed input gain vector ($\mathrm{K\,m^2/J}$)
B_i	radiosity ($\mathrm{W/m^2}$)
c_j	specific heat capacity ($\mathrm{J/(kg\,K)}$)
$\mathcal{D}_j$	differential operator of heat conduction equation ($\mathrm{W/m^3}$)
D	set of allowed transformed state vectors (K)
D_j	thickness of slab (m)
$\boldsymbol{E}$	vector of black body emissive powers ($\mathrm{W/m^2}$)
$\boldsymbol{e}$, $\boldsymbol{e}_j$, $\boldsymbol{e}^s$	control errors (K)
$\boldsymbol{H}$	vector of irradiances ($\mathrm{W/m^2}$)
H	number of basis functions

*Corresponding author. *Tel.:* +43 1 58801 77629, *fax:* +43 1 58801 37699.
Email address: `andreas.steinboeck@tuwien.ac.at` (A. Steinboeck)

Postprint of article accepted for publication in International Journal of Heat and Mass Transfer *July 8, 2010*

Post-print version of the article: A. Steinboeck, D. Wild, T. Kiefer, and A. Kugi, "A mathematical model of a slab reheating furnace with radiative heat transfer and non-participating gaseous media", *International Journal of Heat and Mass Transfer*, vol. 53, no. 25-26, pp. 5933–5946, 2010. DOI: 10.1016/j.ijheatmasstransfer.2010.07.029
The content of this post-print version is identical to the published paper but without the publisher's final layout or copy editing.

H_i	irradiance ($\mathrm{W/m^2}$)
$h_{j,i}$	basis function ($-$)
$\boldsymbol{I}$	identity matrix ($-$)
i	index (usually of furnace zone or surface section)
J	set of indices of currently reheated slabs
j	(usually) index of slab
j_{end}	index of last slab that was pushed into the furnace
j_{start}	index of next slab to be withdrawn from the furnace
k	(usually) discrete time index
k_1, k_2, k_3	constants ($-$)
L^2	space of square integrable functions
L_j	length of slab (m)
l	discrete time index
$\boldsymbol{M}^{\mp}$	matrix mapping slab states to surface temperatures ($-$)
N	number of surface sections
$N_z^{\mp}$	number of furnace zones
N^s	total number of considered slabs
N_s	number of currently reheated slabs
$\boldsymbol{P}$, $\boldsymbol{p}$	positive definite matrices ($-$)
$\boldsymbol{P}_z^{\mp}$, $\boldsymbol{P}_s^{\mp}$	matrices for computing heat flux densities ($\mathrm{W/(m^2\,K^4)}$)
$\boldsymbol{Q}$	vector of heat flows (W)
$\boldsymbol{q}^{\mp}$	vector of heat flux densities ($\mathrm{W/m^2}$)
Q_i	heat flow (W)
q_j	heat flux density ($\mathrm{W/m^2}$)
$q_j^{\mp}$	heat flux density into slab surface ($\mathrm{W/m^2}$)
$\boldsymbol{S}$	vector of surface areas ($\mathrm{m^2}$)
S_i	surface area ($\mathrm{m^2}$)
$S_j^{\mp}$	slab surface area ($\mathrm{m^2}$)
$s_{i,j}$	distance between surfaces (m)
$\overline{\boldsymbol{SS}}$	matrix of total exchange areas ($\mathrm{m^2}$)
$\overline{\boldsymbol{ss}}$	matrix of direct exchange areas ($\mathrm{m^2}$)
$\overline{S_iS_j}$	total exchange area ($\mathrm{m^2}$)
$\overline{s_is_j}$	direct exchange area ($\mathrm{m^2}$)
$\boldsymbol{T}_z^{\mp}$	vector of zone temperatures (K)
$\tilde{\boldsymbol{T}}_z^{\mp}$	reference zone temperature trajectory (K)
T	temperature (K)
T_j	slab temperature (K)
$\bar{T}_{j,exit}$	mean value of final slab temperature (K)
$T_{z,i}^{\mp}$	temperature of furnace zone i (K)
t	time (s)
$t_{j,exit}$	time when slab is withdrawn from furnace (s)
t_k	sampling instant (s)
t_l^s	time of slab movement (s)
$\boldsymbol{V}$	transformation matrix ($-$)
V	Sobolev space
v	trial function ($-$)
W, W^s, w	Lyapunov functions ($\mathrm{K^2}$)
W_j	width of slab (m)
$\boldsymbol{x}$, $\boldsymbol{x}_j$	state vectors (K)
$\hat{\boldsymbol{x}}$	estimated state vector (K)

Post-print version of the article: A. Steinboeck, D. Wild, T. Kiefer, and A. Kugi, "A mathematical model of a slab reheating furnace with radiative heat transfer and non-participating gaseous media", *International Journal of Heat and Mass Transfer*, vol. 53, no. 25-26, pp. 5933–5946, 2010. DOI: 10.1016/j.ijheatmasstransfer.2010.07.029
The content of this post-print version is identical to the published paper but without the publisher's final layout or copy editing.

$\tilde{\boldsymbol{x}}$ reference trajectory of state vector (K)
x, y, z Lagrangian spatial coordinates (m)
$\boldsymbol{z}$, $\boldsymbol{z}_j$ transformed state vectors (K)
z_j position of slab (m)

Greek symbols

$\delta_{i,j}$ Kronecker delta
Δt_k sampling period (s)
$\Delta t_{\min}$, $\Delta t_{\min,l}$ minimum time periods occurring in the stability analysis (s)
$\boldsymbol{\varepsilon}$ vector of emittances (−)
ε emittance (−)
$\varepsilon_j^{\mp}$ emittance of slab surface (−)
λ_j thermal conductivity (W/(m K))
$\mu_{\min}$, $\mu_{\max}$ minimum and maximum eigenvalue
ρ_j mass density (kg/m^3)
σ Stefan-Boltzmann constant (W/(m^2 K^4))
θ_i angle of incidence (rad)

Subscripts

$_0$ initial value
$_h$ finite dimensional approximation
$_k$ corresponding to t_k
$_s$ corresponding to currently reheated slabs
$_z$ corresponding to furnace zones

Superscripts

^{1} corresponding to t_k
^{2} corresponding to t_{k+1}
$^-$ bottom half of furnace
$^+$ top half of furnace
^{s} corresponding to all considered slabs

1. Introduction

1.1. Slab reheating furnaces

In the steel industry, furnaces are used for reheating or heat treatment of steel products. Typical examples are longitudinal reheating furnaces which continuously reheat semi-finished steel blocks to a temperature that is appropriate for processing in the rolling mill. The steel blocks are successively moved through the furnace interior, where fuel-fired burners serve as heat sources. This paper refers to the whole class of semi-finished products that can be processed in such furnaces, e. g., slabs, billets, or bars. Controlling the furnace can be a demanding process, because the products may vary in size, metallurgic properties, initial temperature, and desired rolling temperature. Since rolling is typically a batch process, the feed of steel blocks from the furnace to the mill stand is discontinuous. A common way of realizing the reheating task is to arrange the steel blocks in a row (or several parallel rows) and to (discontinuously) move them through a longitudinal furnace by some transport mechanism. In a *pusher-type slab reheating furnace*, as outlined in Figure 1, a hydraulically or electromechanically operated ram pushes a row of slabs through the furnace in an event-driven manner. Inside the furnace, the slabs slide on skids such that they can be heated from the top and the bottom side.

Post-print version of the article: A. Steinboeck, D. Wild, T. Kiefer, and A. Kugi, "A mathematical model of a slab reheating furnace with radiative heat transfer and non-participating gaseous media", *International Journal of Heat and Mass Transfer*, vol. 53, no. 25-26, pp. 5933–5946, 2010. DOI: 10.1016/j.ijheatmasstransfer.2010.07.029
The content of this post-print version is identical to the published paper but without the publisher's final layout or copy editing.

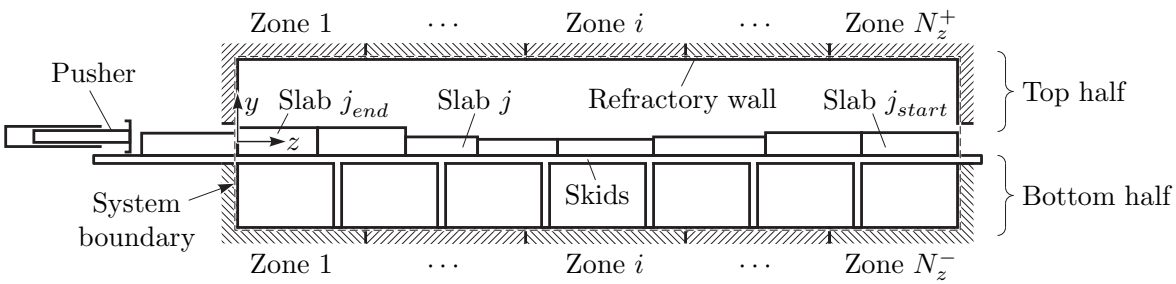

Figure 1: Sectional view of a pusher-type slab reheating furnace.

The temperature profile of the slabs—a system quantity of paramount importance—is not accessible to measurements. The slab surface temperature may be measured by pyrometry at discrete points but the reliability of this method is questionable because of the harsh and irregular conditions of both the furnace interior and the slab surfaces [34]. A common approach of furnace temperature measurements is to equip the refractory furnace wall with shielded thermocouples. Although this paper is focused on a pusher-type slab reheating furnace, the results can be straightforwardly transferred to other furnace types, e. g., *walking-beam furnaces*, where the steel blocks are alternately carried by beams that are slowly moving back and forth.

1.2. Control task

From a system-theoric point of view, pusher-type slab reheating furnaces are nonlinear, distributed-parameter systems with multiple inputs and outputs and discontinuous time dependence. The *fuel* and *air supplies of burners* represent the physical control inputs of the furnace. To simplify the control task, burners may be grouped and jointly regulated. Therefore, it is reasonable to divide the furnace volume conceptually into several zones. Additionally, the *slab movement* and the *order of slabs* may be governed by some supervisory plant scheduling algorithm, implying that these system inputs generally cannot be defined independently from other plant components, e. g., the rolling mill. Therefore, the schedule of slabs is frequently preset by supervisory plant control. There are multiple, sometimes antagonistic control *objectives*:

- Minimum deviation between the desired and the realized final slab temperature profiles
- Maximum throughput of slabs in the furnace
- Minimum specific energy consumption $= \dfrac{\text{Energy supplied by fuel}}{\text{Mass of reheated material}}$
- Minimum loss of material through oxidization (scale formation)
- Minimum decarburization depth which influences the mechanical properties of the products

These objectives are accompanied by a number of operational *constraints*. Some examples are given in the following.

- Construction and geometry of the furnace including type and arrangement of heat sources (burners) and location of heat sinks (slabs, openings, skids, etc.)
- Protection of the furnace against immoderate wear
- Bounds on the temperature of the furnace walls in order to protect them from damage
- Initial slab temperatures
- Metallurgical constraints of the slab temperature trajectory

Post-print version of the article: A. Steinboeck, D. Wild, T. Kiefer, and A. Kugi, "A mathematical model of a slab reheating furnace with radiative heat transfer and non-participating gaseous media", *International Journal of Heat and Mass Transfer*, vol. 53, no. 25-26, pp. 5933–5946, 2010. DOI: 10.1016/j.ijheatmasstransfer.2010.07.029
The content of this post-print version is identical to the published paper but without the publisher's final layout or copy editing.

- Unforeseen standstills or delays caused by upstream or downstream process steps

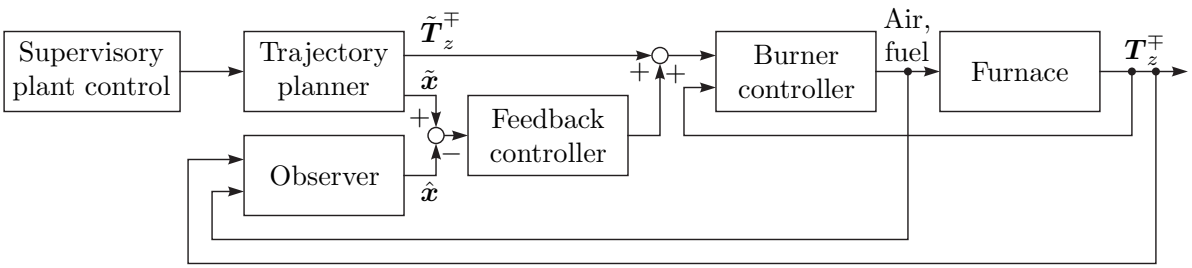

Figure 2: Control scheme of a slab reheating furnace.

The control task may be complicated by non-uniformities of the steel products in terms of initial temperature, desired final temperature, geometry, material, available reheating time, and monetary value (cf. [15, 32, 34]). Considering the complexity of the control task, it is reasonable to follow a *model-based* control approach and to design control systems with *cascaded control loops* [5, 15, 18, 24, 36, 43]. Figure 2 shows an outline of a possible control scheme which is appropriate for non-steady-state operation.

Supervisory plant control provides data of the slabs to be reheated and the production schedule, i. e., path-time diagrams of the slabs. Utilizing this information, a trajectory planner designs reference state trajectories $\tilde{\boldsymbol{x}}(t)$ and corresponding control inputs $\tilde{\boldsymbol{T}}_z^{\mp}(t)$ for the subordinate burner controllers. In this paper, quantities belonging to the bottom and the top half of the furnace (cf. Figure 1) are designated by the superscripts $^-$ and $^+$, respectively. $\boldsymbol{T}_z^{\mp}(t)$ are the measurement values of the thermocouples in the furnace. These temperatures are controlled by an inner control loop, e. g., PI controllers which regulate the supply of air and fuel [5, 15, 18, 43]. An observer provides the estimate $\hat{\boldsymbol{x}}(t)$ of the system state $\boldsymbol{x}(t)$, which cannot be measured. Finally, a feedback controller corrects the planned trajectories $\tilde{\boldsymbol{T}}_z^{\mp}(t)$ to account for model inaccuracies and unforeseen disturbances.

1.3. Temperature tracking

Since the slab temperatures are generally not accessible to measurements, their state variables need to be estimated. To this end, an observer, based on a *sufficiently* accurate mathematical model, may be used. The term *sufficiently* has to be specified on a case by case basis. The considered control scheme uses an extended Kalman filter (see [41] for more details), which was derived from an elaborate mathematical model published in [40]. This model may also be utilized for simulation purposes, for instance to verify the design of the trajectory planner or the feedback controller.

1.4. Motivation for a reduced furnace model

Similar to other process control applications, controlling a slab reheating furnace includes tasks like

- trajectory planning,
- optimization, and
- control, e. g., model predictive control or state feedback control,

Post-print version of the article: A. Steinboeck, D. Wild, T. Kiefer, and A. Kugi, "A mathematical model of a slab reheating furnace with radiative heat transfer and non-participating gaseous media", *International Journal of Heat and Mass Transfer*, vol. 53, no. 25-26, pp. 5933–5946, 2010. DOI: 10.1016/j.ijheatmasstransfer.2010.07.029
The content of this post-print version is identical to the published paper but without the publisher's final layout or copy editing.

usually under the constraints defined by some plant scheduling algorithm. These tasks are characterized by the need for tailored mathematical models (cf. [25]), which are both computationally inexpensive as well as dependable in terms of accuracy and convergence. Fast computation is an important issue, particularly for optimization tasks.

The slab reheating furnace considered in this paper has been in operation for many years and was analyzed in detail by *Wild et al.* [40]. Because of economical reasons and a growing range of products, it is planned to modernize the existing control system. However, in terms of complexity and computational costs, the elaborate model presented in [40] is too demanding for the above listed functions.

Therefore, a *reduced* model is derived, which allows to compute the transient temperature field in the steel slabs, where the radiative heat fluxes inside the furnace serve as boundary conditions. The reduced model represents a balance between accuracy and computational requirements. In view of the control objectives described in Section 1.2, the performance of the reheating furnace is likely to benefit from the introduction of a reduced mathematical model. However, since the proposed model does neither account for the total energy balance of the furnace system nor for scale formation, it is *not* capable of furnishing *quantitative* results on the supplemental control objectives minimum specific energy consumption and minimum loss of material.

1.5. Existing furnace models

Due to the large number of existing mathematical models of slab reheating furnaces, a comprehensive overview of relevant publications would exceed the scope of this paper. Hence, the following outline of the extensive literature can only serve as a possible starting point for further exploration. Computational fluid dynamics models have been left out of account since their mathematical complexity is in conflict with the intended application.

Generally, the models may be distinguished based on the incorporated physical theory. Like in this analysis, so-called *white box models* [36] are adopting the fundamental equations of physical phenomena, such that model parameters are directly assignable to physical quantities of the real system. In contrast, *black box models* (or gray box models) [36] utilize generic structures from system identification theory, which generally does not allow direct physical interpretations. Especially, if physical effects are indistinct or affected by unknown disturbances, the black box approach may be a better choice than physics-based modeling.

Furnace models for steady-state operation as presented in [3, 4, 13, 22] are usually computationally inexpensive, which makes them suitable for optimization tasks. Note that the assumption of steady-state operation requires constant slab velocity or at least constant pushing periods. Then, the slab temperature trajectory is effectively a function of the longitudinal coordinate z of the furnace (cf. Figure 1).

In many studies, e. g., [5, 15, 16, 18, 24, 32, 35, 36, 40, 42, 43], the temperature profile inside the slabs is assumed as 1-dimensional in the vertical direction y. Section 3.1 briefly reflects on the conditions that justify this assumption. Other furnace models like [2, 3, 4, 7, 9, 22, 25, 26, 32] provide for a 2-dimensional temperature distribution in the slabs. This may allow studying the influence of skids on the inhomogeneity of the slab temperature profile. In [13, 20], even the full 3-dimensional temperature field is simulated.

Post-print version of the article: A. Steinboeck, D. Wild, T. Kiefer, and A. Kugi, "A mathematical model of a slab reheating furnace with radiative heat transfer and non-participating gaseous media", *International Journal of Heat and Mass Transfer*, vol. 53, no. 25-26, pp. 5933–5946, 2010. DOI: 10.1016/j.ijheatmasstransfer.2010.07.029
The content of this post-print version is identical to the published paper but without the publisher's final layout or copy editing.

However, there are also lumped-parameter models where each slab is represented in the state vector by its mean temperature only, see for instance [16, 23, 24, 29].

Most frequently, the heat conduction problem is solved by means of the finite difference method (cf. [2, 3, 4, 7, 9, 13, 20, 22, 24, 25, 35, 36, 40, 43]). An alternativ approach was chosen in [42], where the method of weighted residuals (collocation method) with up to 5 polynomial trial functions was applied. Only a few authors account for the temperature dependence of material parameters, e. g., [3, 5, 9, 20, 24, 35, 40]. The problem of temperature-dependent material behavior will be touched upon in Section 3.1.

The method of computing the heat flux into the slabs is another distinguishing feature of furnace models. In some respect any model accounts for the radiative heat transfer into the slabs, but many authors (cf. [3, 4, 5, 7, 15, 16, 23, 29, 35, 36, 42, 43]) neglect the radiative exchange in longitudinal direction z of the furnace. Then, if the bulk gas flow inside the furnace is not taken into account, there is no thermodynamic interaction between the slabs. This approach yields a particularly simple mathematical description, since the dynamic models of the slabs are—apart from the fact that they share some inputs—decoupled.

A more elaborate furnace model is obtained if a full energy balance supplements the computation of radiative heat transfer, which then facilitates the evaluation of the system in terms of specific energy consumption and efficiency. The combustion process and the resulting gas flow towards the funnel are addressed in [2, 7, 23, 31, 35, 40, 42, 43]. An in-depth treatise of the matter can be found in [3], where the position of burner flames and even a recirculating flow component, which opposes the bulk flow, are modeled. The consideration of convective heat transfer between the gas flow and the surfaces is reported in [2, 3, 16, 20, 25, 29, 31, 35].

A system identification method (black box model) is proposed in [18]. Step response experiments were carried out on the real furnace system to provide data for non-parametric system identification with a discrete-time autoregressive model with exogenous input (ARX) enhanced by time-delay behavior. Moreover, ARX models for both the furnace temperatures and the slab temperatures are reported in [5]. Semi-empirical models for the dynamic behavior of the furnace temperatures with the fuel supply rates as inputs are presented in [23, 36]. Another identification model for the furnace temperatures that is suitable for parameter estimation by means of an ARX, finite impulse response, or Box-Jenkins structure is described in [33]. The stochastic model proposed in [16] avoids solving the heat conduction equation by simulating the heat exchange processes as random motions of heat carriers. These black or gray box approaches usually render physical modeling of dynamic processes in the furnace unnecessary.

1.6. Contents

The paper is organized as follows: After an introduction of some basic nomenclature, Section 3 concentrates on the heat conduction problem for a single slab with nonlinear material parameters. The heat conduction equation is solved by the Galerkin method and integrated to obtain a discrete-time representation. In Section 4, the analysis proceeds with the radiative heat exchange inside a multi-surface enclosure filled with a non-participating gaseous medium. Then, the results are transferred to the considered furnace system, which yields the requested reduced state space model given in Section 5. The theoretical part is concluded with a brief discussion about the stability of the system under open-loop control. Finally, Section 7 presents a first comparison between measurement data acquired from the real system and simulation

Post-print version of the article: A. Steinboeck, D. Wild, T. Kiefer, and A. Kugi, "A mathematical model of a slab reheating furnace with radiative heat transfer and non-participating gaseous media", *International Journal of Heat and Mass Transfer*, vol. 53, no. 25-26, pp. 5933–5946, 2010. DOI: 10.1016/j.ijheatmasstransfer.2010.07.029
The content of this post-print version is identical to the published paper but without the publisher's final layout or copy editing.

results. Throughout the paper, an attempt is made to provide at least the most fundamental equations necessary to review and utilize the proposed modeling method.

2. Slab management, geometry, and position

Throughout this analysis, a furnace with one row of slabs is considered. If a furnace contains two or more rows, averaging techniques are recommended. The slab index $j \in \mathbb{N}$ uniquely identifies each slab. All slabs $j \in J = \{j_{start}, j_{start}+1, \ldots, j_{end}\}$ are currently inside the furnace, where j_{start} designates the next slab to be withdrawn from the furnace and j_{end} the last slab that was pushed in. Therefore, j_{start} and j_{end} are updated according to $j_{start} = j_{start} + 1$ and $j_{end} = j_{end} + 1$ every time a slab leaves and enters the furnace, respectively. Let t_l^s with $l \in \mathbb{N}$ mark the time of such events. Likewise, the number of slabs $N_s = |J|$ in the furnace is updated at t_l^s. In the global frame of reference, the center of the slab j has the

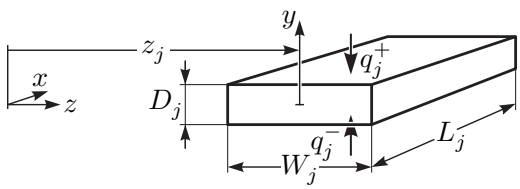

Figure 3: Geometry and position of slab j.

current z-position z_j, as indicated in Figure 3. Slabs can only be moved in positive z-direction. Moreover, let y be a *local* coordinate in vertical direction, which is 0 at the center of the respective slab j. The third spatial coordinate x, defining the lateral direction of the furnace, is not used, because only a 2-dimensional problem is considered. Hence, all variables are assumed to be invariant with respect to x, i. e., the furnace is infinitely wide, and the slabs are infinitely long. The slab j has the thickness D_j in y-direction, the width W_j in z-direction, and the length L_j in x-direction.

3. Conductive heat transfer in a slab

This section addresses the heat balance and the heat conduction problem for a single slab j. As mentioned in Section 1.5, most published furnace models apply the finite difference method for discretization of the spatial domain. However, here, the Galerkin method is used, because it yields a low-dimensional mathematical model that is particularly suitable for control purposes as demonstrated in [37]. Moreover, an implicit time integration scheme is proposed to discretize the time domain, as required for computer implementations.

3.1. Heat conduction problem with Neumann boundary conditions

Let $T_j(y,t) > 0$ be the absolute temperature field in the slab j defined along the vertical spatial dimension y with $y \in [-D_j/2, D_j/2]$, as shown in Figure 3. Here, y is a Lagrangian coordinate. Since the aspect ratio of the slab is usually characterized by $L_j \gg D_j$ and $B_j \gg D_j$, independence of $T_j(y,t)$ from both x and z is a reasonable approximation. The heat flux $q_j(y,t)$ inside the solid is determined by the properties of the

Post-print version of the article: A. Steinboeck, D. Wild, T. Kiefer, and A. Kugi, "A mathematical model of a slab reheating furnace with radiative heat transfer and non-participating gaseous media", *International Journal of Heat and Mass Transfer*, vol. 53, no. 25-26, pp. 5933–5946, 2010. DOI: 10.1016/j.ijheatmasstransfer.2010.07.029
The content of this post-print version is identical to the published paper but without the publisher's final layout or copy editing.

material, the temperature gradient, and the boundary conditions at $y = -{}^{D_j}/2$ and $y = {}^{D_j}/2$. Therefore, *Fourier*'s law $q_j(y,t) = -\lambda_j \partial T_j(y,t)/\partial y$ and the differential operators

$$\mathcal{D}_j(T_j) := \rho_j c_j \frac{\partial T_j}{\partial t} + \frac{\partial q_j}{\partial y} = \rho_j c_j \frac{\partial T_j}{\partial t} - \frac{\partial}{\partial y}\left(\lambda_j \frac{\partial T_j}{\partial y}\right) \tag{1a}$$

$$\mathcal{B}_j^{\mp}(T_j) := \mp q_j\left(\mp {}^{D_j}/2, t\right) \mp \lambda_j \left.\frac{\partial T_j}{\partial y}\right|_{y=\mp D_j/2} = -q_j^{\mp}(t) \mp \lambda_j \left.\frac{\partial T_j}{\partial y}\right|_{y=\mp D_j/2} \tag{1b}$$

can be used for defining the heat conduction process by the diffusion law [1, 19]

$$\mathcal{D}_j(T_j(y,t)) = 0 \qquad y \in \left(-{}^{D_j}/2, {}^{D_j}/2\right),\ t > t_0 \tag{1c}$$

with initial conditions

$$T_j(y,t_0) = T_{j,0}(y) \qquad y \in \left[-{}^{D_j}/2, {}^{D_j}/2\right] \tag{1d}$$

and Neumann boundary conditions

$$\mathcal{B}_j^{-}(T_j(y,t)) = \mathcal{B}_j^{+}(T_j(y,t)) = 0 \qquad t > t_0. \tag{1e}$$

It is assumed that $T_j(y,t)$ always satisfies the differentiability requirements induced by the operators $\mathcal{D}_j$ and $\mathcal{B}_j^{\mp}$. The heat inputs $q_j^-(t)$ and $q_j^+(t)$ define the heat exchange between the solid and its environment. They may depend on the surface temperatures $T_j(-{}^{D_j}/2, t)$ and $T_j({}^{D_j}/2, t)$, respectively. Here, the heat conduction problem is given in its *differential* (strong) formulation. Section 3.2 touches upon the corresponding *integral* (weak) formulation.

In (1), ρ_j represents the mass density, which may depend on y only. The specific heat capacity c_j and the thermal conductivity λ_j may depend on y or T_j or both. In fact, the material behavior may vary with the coordinate y if multi-layer steel products are considered. However, in this analysis, a homogeneous material, i. e., independence of the parameters from y, is stipulated. Moreover, possible dependence of the parameters on the history of T_j is disregarded, i. e., c_j and λ_j may only depend on the current local temperature. An example for the dependence of the parameters on the local temperature $T_j(y,t)$ is given in Figure 4 for standard steel (0.1 % carbon). The salient peak of c_j corresponds to a phase transition. Throughout this paper, if temperature dependence is allowed for, data from Figure 4 is used. The reference [14] provides more information on the temperature dependence of material parameters.

The nonlinear temperature dependence of c_j and λ_j renders the partial differential equation (1) nonlinear, which complicates its solution, especially if solution techniques based on the weak formulation are applied. In [37], a method was proposed which allows to accurately account for the nonlinearity by replacing the temperature as a state variable with a transformed quantity proportional to the specific enthalpy. A simpler but less precise approach is outlined in the following.

Post-print version of the article: A. Steinboeck, D. Wild, T. Kiefer, and A. Kugi, "A mathematical model of a slab reheating furnace with radiative heat transfer and non-participating gaseous media", *International Journal of Heat and Mass Transfer*, vol. 53, no. 25-26, pp. 5933–5946, 2010. DOI: 10.1016/j.ijheatmasstransfer.2010.07.029
The content of this post-print version is identical to the published paper but without the publisher's final layout or copy editing.

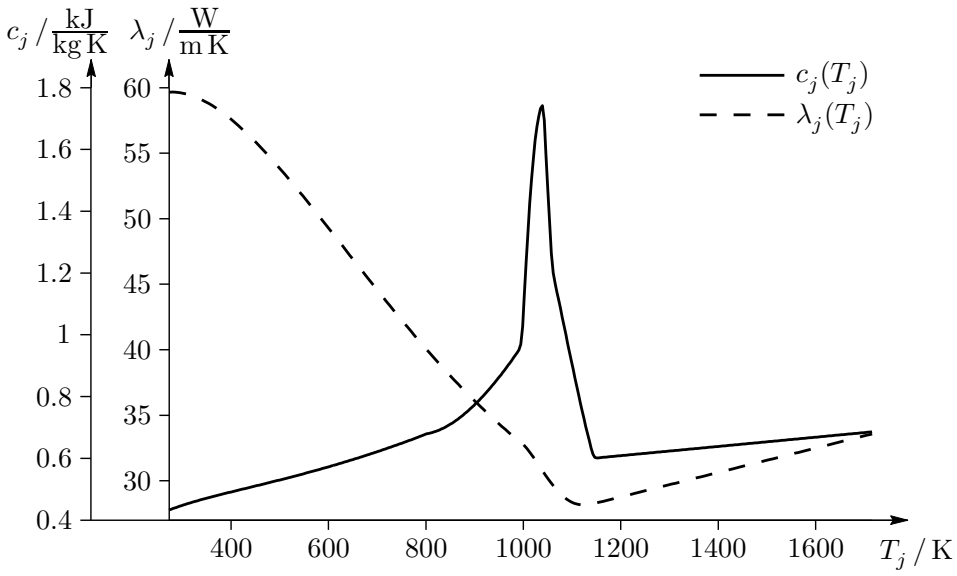

Figure 4: Temperature-dependent material parameters for standard steel with 0.1 % carbon (data adapted from [14]).

3.2. Weighted residual method

Assume for the time being that c_j and λ_j are independent of the temperature T_j. Later, some measures will be taken to compensate at least partially for the error introduced by this assumption. Then, $\mathcal{D}_j$ from (1a) is a linear operator. Consider the Sobolev space $V := H^1(-D_j/2, D_j/2)$ and the bilinear form

$$a(v_1, v_2) := \int_{-D_j/2}^{D_j/2} v_1 v_2 \mathrm{d}y \ : \ V \times V \to \mathbb{R}. \tag{2}$$

Using *any* trial function $v(y) \in V$ and *any* scalars $v^-, v^+ \in \mathbb{R}$, the identity

$$a(v(y), \mathcal{D}_j(T_j(y,t))) + v^- \mathcal{B}_j^-(T_j(y,t)) + v^+ \mathcal{B}_j^+(T_j(y,t)) = 0 \qquad t > t_0 \tag{3a}$$

must hold. Here, $\mathcal{D}_j(T_j(y,t)) \in L^2(-D_j/2, D_j/2)$ is required, where $L^2(-D_j/2, D_j/2)$ is the space of square integrable functions on the interval $(-D_j/2, D_j/2)$. In the usual way (cf. [30]), integration by parts yields

$$\begin{aligned} 0 = \rho_j c_j a\left(v(y), \frac{\partial T_j(y,t)}{\partial t}\right) + \lambda_j a\left(\frac{\partial v(y)}{\partial y}, \frac{\partial T_j(y,t)}{\partial y}\right) + \left(v^+ - v\left(D_j/2\right)\right) \lambda_j \left.\frac{\partial T_j(y,t)}{\partial y}\right|_{y=D_j/2} - v^+ q_j^+(t) \\ - \left(v^- - v\left(-D_j/2\right)\right) \lambda_j \left.\frac{\partial T_j(y,t)}{\partial y}\right|_{y=-D_j/2} - v^- q_j^-(t) \qquad t > t_0. \end{aligned} \tag{3b}$$

The formulations (1) and (3b) are equivalent, apart from the fact that (3b) induces less restrictive requirements on the differentiability of $T_j(y,t)$ with respect to y.

The idea of the *weighted residual method* is to find an approximate solution by weakening the condition that (3) must be satisfied for *any* trial function $v(y) \in V$ and *any* scalars $v^-, v^+ \in \mathbb{R}$. For the approximation, it suffices if (3) holds for *any* $v(y) \in V_h \subseteq V$ and *any* $v^-, v^+ \in V_h^{\mp} \subseteq \mathbb{R}$, where V_h is a finite dimensional subspace. Moreover, (3b) can be simplified by means of the choice $v^{\mp} = v(\mp D_j/2)$. As demonstrated in [44],

Post-print version of the article: A. Steinboeck, D. Wild, T. Kiefer, and A. Kugi, "A mathematical model of a slab reheating furnace with radiative heat transfer and non-participating gaseous media", *International Journal of Heat and Mass Transfer*, vol. 53, no. 25-26, pp. 5933–5946, 2010. DOI: 10.1016/j.ijheatmasstransfer.2010.07.029
The content of this post-print version is identical to the published paper but without the publisher's final layout or copy editing.

this reasonable simplification is particularly useful for Neumann boundary conditions. It is, therefore, used throughout the following analysis.

3.3. Galerkin method

Generally, the choice of V_h is left to the user. A well-known type of the weighted residual approach is the *Galerkin method* (cf. [8, 30]). It suggests to approximate the exact solution $T_j(y,t)$ by

$$T_{h,j}(y,t) = \sum_{i=1}^{H} x_{j,i}(t) h_{j,i}(y) \tag{4}$$

with H basis functions $h_{j,i}(y) \in V_h := \operatorname{span}\{h_1(y), h_2(y), \ldots, h_H(y)\} \subseteq V$, which are also used as trial functions $v(y)$ in (3). I. e., the trial functions $v(y)$ and the approximate solution $T_{h,j}(y,t)$ are taken from the same finite dimensional space V_h. In (4), the time dependence of T_j is reflected by the so-called Galerkin coefficients $x_{j,i}(t)$, which can be summarized in the vector $\boldsymbol{x}_j(t) = [x_{j,1}(t), x_{j,2}(t), \ldots, x_{j,H}(t)]^\mathsf{T}$. To render the linear combination (4) unique, the trial functions $h_{j,i}(y)$ have to be linearly independent. In case of $q_j^-(t) = 0$ or $q_j^+(t) = 0$ or both, V_h can be chosen such that the homogeneous boundary conditions are automatically satisfied by $T_{h,j}(y,t)$. However, for the considered problem, the boundary conditions are generally inhomogeneous.

Evaluation of (3b) by sequential replacement of $v(y)$ with the H trial functions $h_{j,i}(y)$ yields an initial-value problem in form of an explicit ODE for the unknown Galerkin coefficients $\boldsymbol{x}_j(t)$. Therefore, $\boldsymbol{x}_j(t)$ are the states of a dynamical system of order H (lumped-parameter system). A reasonable strategy for obtaining the initial values $\boldsymbol{x}_j(t_0) = \boldsymbol{x}_{j,0}$ is to minimize the deviation between $T_{h,j}(y,t_0)$ and the given initial temperature profile $T_{j,0}(y)$ weighted with the trial functions $h_{j,i}(y)$ by claiming $a(h_{j,i}(y), T_{h,j}(y,t_0) - T_{j,0}(y)) = 0$ $\forall\, i \in \{1, 2, \ldots, H\}$. Insertion of (4) and utilization of the linearity of the operator $a(v_1, v_2)$ from (2) yield the linear equation

$$\left[a(h_{j,i}(y), h_{j,k}(y))\right]_{i=1\ldots H, k=1\ldots H} \boldsymbol{x}_{j,0} = \left[a(h_{j,i}(y), T_{j,0}(y))\right]_{i=1\ldots H}. \tag{5}$$

Since linear independence of the basis functions $h_{j,i}(y)$ was assumed, (5) can be straightforwardly solved for the initial state $\boldsymbol{x}_{j,0}$. In the sequel, the proposed approach is explained with a three-dimensional *orthogonal* basis

$$h_{j,1}(y) = 1, \qquad h_{j,2}(y) = \frac{2y}{D_j}, \qquad h_{j,3}(y) = \left(\frac{2y}{D_j}\right)^2 - \frac{1}{3}, \tag{6}$$

i. e., $H = 3$ and $T_{h,j}(y,t)$ is a quadratic polynomial in y. This choice allows a straightforward interpretation of the Galerkin coefficients $\boldsymbol{x}_j$: $x_{j,1}$ is the slab mean temperature, $x_{j,2}$ defines the asymmetry of the temperature profile $T_{h,j}(y,t)$, and $x_{j,3}$ is the transient temperature inhomogeneity, which depends on the relation between the total heat flux into the slab and the heat conductivity inside the slab. Thermal expansions corresponding to $x_{j,2}$ cause the slab to bend, whereas those corresponding to $x_{j,3}$ cause thermal stresses.

The rationale for the choice (6) is that—given the right initial condition $T_{j,0}(y)$—it would allow an *exact* solution of (1) if $q_j^-(t)$ and $q_j^+(t)$ were constant. For an arbitrary initial condition $T_{j,0}(y)$, the error

Post-print version of the article: A. Steinboeck, D. Wild, T. Kiefer, and A. Kugi, "A mathematical model of a slab reheating furnace with radiative heat transfer and non-participating gaseous media", *International Journal of Heat and Mass Transfer*, vol. 53, no. 25-26, pp. 5933–5946, 2010. DOI: 10.1016/j.ijheatmasstransfer.2010.07.029
The content of this post-print version is identical to the published paper but without the publisher's final layout or copy editing.

would be transient. As reported in [37], the chosen trial functions are an acceptable compromise between computational effort and achieved accuracy. Results for $H > 3$ are shown in [37].

Substitution of (6) and (4) into (3b) for $v = h_1$, $v = h_2$, and $v = h_3$ with $v^{\mp} = v(\mp {}^{D_j}/_2)$ yields the so far linear ODE

$$\dot{\boldsymbol{x}}_j(t) = \boldsymbol{a}_j \boldsymbol{x}_j(t) + \boldsymbol{b}_j^- q_j^-(t) + \boldsymbol{b}_j^+ q_j^+(t) \qquad t > t_0 \tag{7a}$$

with the initial value $\boldsymbol{x}_j(t_0) = \boldsymbol{x}_{j,0}$ from (5) and the expressions

$$\boldsymbol{a}_j = -\frac{12\lambda_j}{\rho_j c_j D_j^2} \operatorname{diag}\{0 \quad 1 \quad 5\}, \qquad \boldsymbol{b}_j^{\mp} = \frac{1}{\rho_j c_j D_j}[1 \quad \mp 3 \quad {}^{15}/_2]^{\mathsf{T}}. \tag{7b}$$

In (7), it is possible to approximately compensate for the ignored temperature dependence of c_j and λ_j by substituting these parameters with weighted mean values

$$\bar{c}_j(\boldsymbol{x}_j) = \frac{a\big(c_j(T_{h,j}), T_{h,j}\big)}{a\big(h_{j,1}, T_{h,j}\big)}, \qquad \bar{\lambda}_j(\boldsymbol{x}_j) = \frac{a\left(\lambda_j(T_{h,j}), \frac{\partial T_{h,j}}{\partial y}\right)}{a\left(h_{j,1}, \frac{\partial T_{h,j}}{\partial y}\right)}. \tag{8}$$

Then, the ODE (7) becomes *nonlinear*. Although, the choice (8) is not well-founded in theory, it yields acceptable results in practice. The reference [37] sheds some light upon the rationale for the approach. When implementing (8), special care should be taken to handle the case of vanishing denominators—a case that is not exceptional.

The heat fluxes $q_j^{\mp}(t)$ in (7a) could be replaced by expressions for the radiative heat exchange between the slab and its environment. However, noting that $q_j^-(t)$ and $q_j^+(t)$ depend in a nonlinear fashion on the surface temperature $T_{h,j}(-{}^{D_j}/_2, t)$ and $T_{h,j}({}^{D_j}/_2, t)$, respectively, a significant nonlinearity would be introduced into (7a). Therefore, to simplify the solution of (7a), the consideration of radiative heat exchange is postponed until a discrete-time system has been obtained. In the sequel, the subscript $_h$ is omitted, because it can be easily inferred from the respective context whether the exact or the approximate solution is meant.

3.4. Discretization of the time domain

An analytical solution of the ODE (7) with c_j and λ_j replaced by $\bar{c}_j(\boldsymbol{x}_j)$ and $\bar{\lambda}_j(\boldsymbol{x}_j)$ from (8), respectively, has not been found. Hence, a computer implementation of the model requires the time domain to be discretized by applying some (approximate) integration algorithm. Any standard numerical ODE solver for explicit initial-value problems should suffice to integrate this ODE. However, the benefit of manual discretization is that usually laborious iterative solver algorithms can be replaced by algebraic difference equations, which allow rapid evaluation. Consider a discretized time domain with sampling instants $t_k \; \forall\, k \in \mathbb{N}$, which do *not* need to be equidistant, and let $\Delta t_k = t_{k+1} - t_k$ be the corresponding sampling period. In order to obtain a discrete representation [10] of the state space system (7) and (8), the input signals $q_j^{\mp}(t)$ can be restricted to a function space that facilitates an analytical integration of the ODE. The zero-order-hold method [10] is a well known example, where only piecewise constant input signals are allowed. More accurate results are obtained by using *piecewise linear* signals which may be *discontinuous* at the

Post-print version of the article: A. Steinboeck, D. Wild, T. Kiefer, and A. Kugi, "A mathematical model of a slab reheating furnace with radiative heat transfer and non-participating gaseous media", *International Journal of Heat and Mass Transfer*, vol. 53, no. 25-26, pp. 5933–5946, 2010. DOI: 10.1016/j.ijheatmasstransfer.2010.07.029
The content of this post-print version is identical to the published paper but without the publisher's final layout or copy editing.

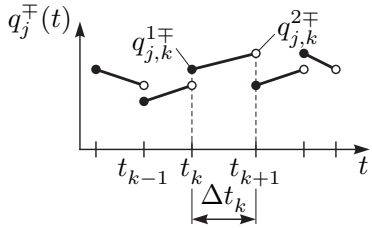

Figure 5: Piecewise linear input signal.

sampling points t_k. Figure 5 shows an example for $q_j^{\mp}(t)$. However, the continuous inputs $q_j^{-}(t)$ and $q_j^{+}(t)$ are generally not equal. They can be expressed as

$$q_j^{\mp}(t) = q_{j,k}^{1\mp}\frac{t_{k+1}-t}{\Delta t_k} + q_{j,k}^{2\mp}\frac{t-t_k}{\Delta t_k} \qquad \text{for} \qquad t_k \le t < t_{k+1}, \tag{9}$$

where $q_{j,k}^{1\mp}$ and $q_{j,k}^{2\mp}$ follow from

$$q_{j,k}^{1\mp} = q_j^{\mp}(t_k), \qquad q_{j,k}^{2\mp} = \lim_{\tau\to 0^-} q_j^{\mp}(t_{k+1}+\tau).$$

To permit a simple analytical solution, it is assumed that $\bar{c}_j(\boldsymbol{x}_j)$ and $\bar{\lambda}_j(\boldsymbol{x}_j)$ take the *constant* values $\bar{c}_j(\boldsymbol{x}_{j,k})$ and $\bar{\lambda}_j(\boldsymbol{x}_{j,k})$ within each time interval $[t_k, t_{k+1})$. Implementing this *approximation*, the integration of (7) with the inputs (9) readily yields the discrete-time system

$$\boldsymbol{x}_{j,k+1} = \boldsymbol{a}_{j,k}\boldsymbol{x}_{j,k} + \boldsymbol{b}_{j,k}^{1-}q_{j,k}^{1-} + \boldsymbol{b}_{j,k}^{1+}q_{j,k}^{1+} + \boldsymbol{b}_{j,k}^{2-}q_{j,k}^{2-} + \boldsymbol{b}_{j,k}^{2+}q_{j,k}^{2+} \tag{10a}$$

with

$$\boldsymbol{a}_{j,k} = \mathrm{e}^{-\frac{12\bar{\lambda}_j(\boldsymbol{x}_{j,k})\Delta t_k}{\rho_j\bar{c}_j(\boldsymbol{x}_{j,k})D_j^2}}\,\mathrm{diag}\,\{0 \quad 1 \quad 5\} \tag{10b}$$

$$\boldsymbol{b}_{j,k}^{1\mp} = \begin{bmatrix} \frac{\Delta t_k}{2\rho_j\bar{c}_j(\boldsymbol{x}_{j,k})D_j} \\ \mp\frac{D_j}{4\bar{\lambda}_j(\boldsymbol{x}_{j,k})}\left(-1+\left(1+\frac{\rho_j\bar{c}_j(\boldsymbol{x}_{j,k})D_j^2}{12\bar{\lambda}_j(\boldsymbol{x}_{j,k})\Delta t_k}\right)\left(1-\mathrm{e}^{\frac{-12\bar{\lambda}_j(\boldsymbol{x}_{j,k})\Delta t_k}{\rho_j\bar{c}_j(\boldsymbol{x}_{j,k})D_j^2}}\right)\right) \\ \frac{D_j}{8\bar{\lambda}_j(\boldsymbol{x}_{j,k})}\left(-1+\left(1+\frac{\rho_j\bar{c}_j(\boldsymbol{x}_{j,k})D_j^2}{60\bar{\lambda}_j(\boldsymbol{x}_{j,k})\Delta t_k}\right)\left(1-\mathrm{e}^{\frac{-60\bar{\lambda}_j(\boldsymbol{x}_{j,k})\Delta t_k}{\rho_j\bar{c}_j(\boldsymbol{x}_{j,k})D_j^2}}\right)\right) \end{bmatrix} \tag{10c}$$

$$\boldsymbol{b}_{j,k}^{2\mp} = \begin{bmatrix} \frac{\Delta t_k}{2\rho_j\bar{c}_j(\boldsymbol{x}_{j,k})D_j} \\ \mp\frac{D_j}{4\bar{\lambda}_j(\boldsymbol{x}_{j,k})}\left(1-\frac{\rho_j\bar{c}_j(\boldsymbol{x}_{j,k})D_j^2}{12\bar{\lambda}_j(\boldsymbol{x}_{j,k})\Delta t_k}\left(1-\mathrm{e}^{\frac{-12\bar{\lambda}_j(\boldsymbol{x}_{j,k})\Delta t_k}{\rho_j\bar{c}_j(\boldsymbol{x}_{j,k})D_j^2}}\right)\right) \\ \frac{D_j}{8\bar{\lambda}_j(\boldsymbol{x}_{j,k})}\left(1-\frac{\rho_j\bar{c}_j(\boldsymbol{x}_{j,k})D_j^2}{60\bar{\lambda}_j(\boldsymbol{x}_{j,k})\Delta t_k}\left(1-\mathrm{e}^{\frac{-60\bar{\lambda}_j(\boldsymbol{x}_{j,k})\Delta t_k}{\rho_j\bar{c}_j(\boldsymbol{x}_{j,k})D_j^2}}\right)\right) \end{bmatrix}. \tag{10d}$$

By virtue of the chosen function space for the inputs $q_j^{\mp}(t)$, the discrete-time system (10) has 4 inputs $(q_{j,k}^{1\mp})$ and $(q_{j,k}^{2\mp})$ whereas the original continuous-time system (7) has just 2 inputs $q_j^{\mp}(t)$. Moreover, (10) is non-causal, since $q_{j,k}^{2\mp}$ occurs at the same time as $\boldsymbol{x}_{j,k+1}$. As a consequence of boundary conditions, $q_{j,k}^{2\mp}$

Post-print version of the article: A. Steinboeck, D. Wild, T. Kiefer, and A. Kugi, "A mathematical model of a slab reheating furnace with radiative heat transfer and non-participating gaseous media", *International Journal of Heat and Mass Transfer*, vol. 53, no. 25-26, pp. 5933–5946, 2010. DOI: 10.1016/j.ijheatmasstransfer.2010.07.029
The content of this post-print version is identical to the published paper but without the publisher's final layout or copy editing.

may depend on $\boldsymbol{x}_{j,k+1}$ such that (10a) constitutes an implicit discrete-time system, as will be shown for the complete furnace model in Section 5.2. The benefit of the proposed integration scheme compared to the classical zero-order-hold method is that complicated input signals $q_j^{\mp}(t)$, e. g., ramps with non-equidistant discontinuities, can be approximated more accurately, see also [37].

4. Radiative heat transfer in the furnace

The input signals $q_j^{\mp}(t)$ of each slab $j \in J$ represent radiative heat fluxes inside the furnace. Radiative heat transfer generally couples the dynamical subsystems of all slabs, because radiation is not just a local phenomenon. Before the *net radiation method* [1, 19, 27] is utilized to model the radiative heat transfer inside the furnace, a few assumptions are made.

4.1. Assumptions

The most basic assumptions about the radiation conditions in the considered furnace are listed in the following. Admittedly, this gives only an incomplete rendering of the sometimes intricate physical details of radiative heat transfer. For an in-depth discussion of the issue, the references [1, 12, 27, 31, 38] may serve as a point of departure.

- Thermal radiation is the only considered mode of heat exchange between the slabs and their environment. Especially, high surface temperatures make thermal radiation the dominant mode of heat exchange [15, 20, 25, 40]. Therefore, other types of heat transfer like *conduction* or *convection* are negligible.
- At any time, the temperature of a participating surface is homogeneously distributed. This postulate seems adequate for slab surfaces. For furnace wall surfaces, however, its validity depends largely on the chosen size of the surface section, the distribution of burners, and the gaseous flow inside the furnace.
- The temperature $T_{z,i}^{\mp}$, which is measured by thermocouples in the furnace zone $i \in \{1, 2, \ldots, N_z^{\mp}\}$, is an intermediate value of the local gas temperature and the surface temperature of the furnace wall. In the proposed model, $T_{z,i}^{\mp}$ is considered to equal the wall surface temperature in zone i. Therefore, $T_{z,i}^{\mp}$ is called the *zone* temperature. It is usually regulated by a burner controller (cf. Figure 2) and serves as an *input* of the model.
- The transmissive properties of the gaseous medium inside the furnace are assumed to be negligible. This assumption is correct if the medium does *not* emit thermal radiation and if rays passing the medium are neither *scattered* nor *absorbed* or *attenuated* [1, 19]. Then, the medium is said to be *non-participating*.

  Evidently, this is a bold approximation since burner flames and flue gases transfer thermal energy to the surfaces inside the furnace *mainly* through radiation and this effect is responsible for the bulk of the heat input into the furnace. To compensate for the error introduced by this approximation, the parameters describing the radiative properties of the participating surfaces are adapted such that $T_{z,i}^{\mp}$ can be regarded as a system input. Hence, $T_{z,i}^{\mp}$ shall incorporate the effects of both the gaseous medium and the furnace wall in zone i. It is emphasized that this yields a fairly imprecise but at least computationally easily manageable model.

Post-print version of the article: A. Steinboeck, D. Wild, T. Kiefer, and A. Kugi, "A mathematical model of a slab reheating furnace with radiative heat transfer and non-participating gaseous media", *International Journal of Heat and Mass Transfer*, vol. 53, no. 25-26, pp. 5933–5946, 2010. DOI: 10.1016/j.ijheatmasstransfer.2010.07.029
The content of this post-print version is identical to the published paper but without the publisher's final layout or copy editing.

- All participating surfaces are ideal diffuse reflectors. Bearing in mind the irregularly textured and mat surfaces of a furnace system, this assumption comes close to reality.
- All participating surfaces behave as gray bodies. For the prevailing temperature range in a furnace, this seems to be an acceptable approximation, which is adopted in most pertinent publications. However, furnace models which explicitly allow for the spectral distribution of thermal radiation are reported in [13, 22, 26].

  Gray bodies have a spectrum that is proportional to that of black bodies with the proportionality coefficient $\varepsilon \in [0, 1]$. The factor ε is known as *emittance*. Black bodies absorb all incident rays ($\varepsilon = 1$), whereas gray bodies partially reflect incident radiation ($\varepsilon < 1$) [1, 19]. In reality, ε may vary with the surface temperature. However, as discussed in [6, 35], the sensitivity of the radiative heat transfer process on variations of ε is only minor, which justifies the disregard of this effect.
- All participating surfaces are opaque.

These stipulations are supplemented by assumptions concerning the geometry of the furnace, which is outlined in Figure 1.

- Both the top and the bottom half of the furnace form a multi-surface enclosure. Radiative heat exchange occurs neither between the furnace environment and the two enclosures nor between the enclosures themselves.
- Since the furnace is considered infinitely wide and the slabs are considered infinitely long, the radiation conditions are invariant with respect to x. The radiation problem can be interpreted as 2-dimensional.
- Skids are ignored when computing the radiative heat exchange. However, it is possible to approximately account for their negative effect on the heat flux into the slabs by choosing the emissivity ε_j^- of the bottom slab surface smaller than the emissivity ε_j^+ of the top slab surface.
- Only the bottom and the top surface of a slab serve as interface for heat exchange between the slab and its environment. Front, back, and lateral slab faces do not participate in the radiative heat exchange process.
- For computing the radiative heat transfer, the thickness of the slabs is not taken into account, i. e., it is assumed that all top slab surfaces are in the same plane. For the bottom slab surfaces, this holds anyway.

4.2. Radiative heat transfer in a multi-surface enclosure

The so-called *zone method* (cf. [17]) furnishes a model of the radiative heat transfer in some gaseous media surrounded by solid surfaces. The net radiation method (cf. [1, 19, 27]) is a simplified version of this theory, applicable to systems with non-participating gaseous media, as assumed in this analysis. Other sources of the following discussion are [27, 28, 31]. The total emissive power of a gray body surface i with area S_i is defined as $\sigma\varepsilon_i T_i^4$, where σ is the Stefan-Boltzmann constant and T_i the absolute temperature of the surface. For black bodies, the well-known *Stefan-Boltzmann* law is obtained by setting $\varepsilon_i = 1$. Let H_i be the flux density of radiative energy which radiates onto the surface S_i, as outlined in Figure 6a). H_i is known as *irradiance*. Moreover, B_i is the flux density of radiation energy departing from the surface i

Post-print version of the article: A. Steinboeck, D. Wild, T. Kiefer, and A. Kugi, "A mathematical model of a slab reheating furnace with radiative heat transfer and non-participating gaseous media", *International Journal of Heat and Mass Transfer*, vol. 53, no. 25-26, pp. 5933–5946, 2010. DOI: 10.1016/j.ijheatmasstransfer.2010.07.029
The content of this post-print version is identical to the published paper but without the publisher's final layout or copy editing.

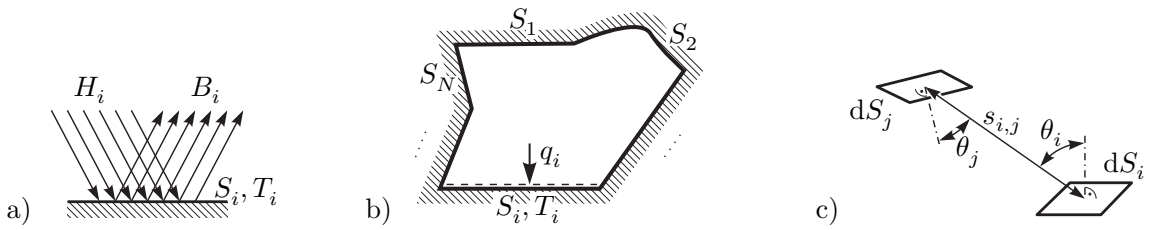

Figure 6: a) Irradiance H_i and radiosity B_i of the surface section S_i, b) multi-surface enclosure, c) geometric relation between two infinitesimal surface sections.

including the reflected fraction of H_i. B_i is known as *radiosity* and follows as

$$B_i = (1 - \varepsilon_i)H_i + \sigma\varepsilon_i T_i^4. \tag{11a}$$

The proportionality coefficient $1 - \varepsilon_i$ refers to *Kirchhoff*'s law of thermal radiation [1, 19] and is called *reflectance*. Drawing up the balance of heat fluxes at the surface i yields the net heat flux density $q_i = H_i - B_i$ into the surface and the corresponding net heat flow

$$Q_i = S_i q_i = S_i(H_i - B_i). \tag{11b}$$

Consider a multi-surface enclosure with N surface zones, as shown in Figure 6b), and let S_i and S_j be the areas of two sections of this enclosure. Hence, $S_j H_j$ is the total radiative energy incident on the surface j. The fraction of $S_j H_j$ that is attributed to the emitting zone i is defined as $\overline{s_i s_j} B_i$ with the so-called *direct exchange area* $\overline{s_i s_j}$ (cf. [12, 17, 27, 28]). It is found by integration over *all possible light beams* traveling from the emitter S_i to the receiver S_j, i. e.,

$$\overline{s_i s_j} := \int_{S_i}\int_{S_j} \frac{\cos(\theta_i)\cos(\theta_j)}{\pi s_{i,j}^2}\mathrm{d}S_j\mathrm{d}S_i. \tag{12}$$

As indicated in Figure 6c), $s_{i,j}$ is the distance between two infinitesimal sections on the surfaces i and j. θ_i and θ_j are the corresponding angles of incidence, i. e., the angles between the light ray and the perpendicular to the surface section. It is emphasized that (12) only holds for non-participating media. The equation can be explained by taking into account that

$$\frac{\cos(\theta_i)\cos(\theta_j)}{\pi s_{i,j}^2}\mathrm{d}S_j$$

is the fraction of the viewing field of $\mathrm{d}S_i$ occupied by $\mathrm{d}S_j$ [27]. Because of the symmetric occurrence of i and j in (12), $\overline{s_i s_j} = \overline{s_j s_i}$, which is known as *reciprocity relation*. Depending on the complexity of the given geometry, the *multiple* integral (12) may be computationally expensive. The problem can be alleviated by assuming a planar configuration, like in this analysis.

To ensure a concise notation, some matrices and vectors are introduced before the balance of radiation

Post-print version of the article: A. Steinboeck, D. Wild, T. Kiefer, and A. Kugi, "A mathematical model of a slab reheating furnace with radiative heat transfer and non-participating gaseous media", *International Journal of Heat and Mass Transfer*, vol. 53, no. 25-26, pp. 5933–5946, 2010. DOI: 10.1016/j.ijheatmasstransfer.2010.07.029
The content of this post-print version is identical to the published paper but without the publisher's final layout or copy editing.

energy in the multi-surface enclosure is drawn up.

$$\overline{\boldsymbol{ss}} = \overline{\boldsymbol{ss}}^{\mathsf{T}} = [\,\overline{s_i s_j}\,]_{i=1\ldots N, j=1\ldots N}\,, \qquad \boldsymbol{S} = [S_1 \quad S_2 \quad \cdots \quad S_N]^{\mathsf{T}}, \qquad \boldsymbol{\varepsilon} = [\varepsilon_1 \quad \varepsilon_2 \quad \cdots \quad \varepsilon_N]^{\mathsf{T}},$$
$$\boldsymbol{B} = [B_1 \quad B_2 \quad \cdots \quad B_N]^{\mathsf{T}}, \qquad \boldsymbol{H} = [H_1 \quad H_2 \quad \cdots \quad H_N]^{\mathsf{T}}, \qquad \boldsymbol{E} = \sigma[T_1^4 \quad T_2^4 \quad \cdots \quad T_N^4]^{\mathsf{T}},$$
$$\boldsymbol{Q} = [Q_1 \quad Q_2 \quad \cdots \quad Q_N]^{\mathsf{T}}$$

Summing up the fractions $\overline{s_i s_j} B_i$ for each surface yields

$$\operatorname{diag}\{\boldsymbol{S}\}\,\boldsymbol{H} = \overline{\boldsymbol{ss}}\boldsymbol{B}. \tag{13a}$$

The counterparts of (11) in matrix notation read as

$$\boldsymbol{B} = (\boldsymbol{I} - \operatorname{diag}\{\boldsymbol{\varepsilon}\})\boldsymbol{H} + \operatorname{diag}\{\boldsymbol{\varepsilon}\}\,\boldsymbol{E} \tag{13b}$$
$$\boldsymbol{Q} = \operatorname{diag}\{\boldsymbol{S}\}\,(\boldsymbol{H} - \boldsymbol{B}). \tag{13c}$$

Elimination of $\boldsymbol{B}$ and $\boldsymbol{H}$ in (13) yields the net heat flows into the surface zones as

$$\boldsymbol{Q} = \left(\overline{\boldsymbol{SS}} - \operatorname{diag}\{\boldsymbol{S}\}\operatorname{diag}\{\boldsymbol{\varepsilon}\}\right)\boldsymbol{E} \tag{14}$$

with the so-called *total exchange areas*

$$\overline{\boldsymbol{SS}} = \left[\,\overline{S_i S_j}\,\right]_{i=1\ldots N, j=1\ldots N} = \operatorname{diag}\{\boldsymbol{S}\}\operatorname{diag}\{\boldsymbol{\varepsilon}\}\left[\operatorname{diag}\{\boldsymbol{S}\} - \overline{\boldsymbol{ss}}\,(\boldsymbol{I} - \operatorname{diag}\{\boldsymbol{\varepsilon}\})\right]^{-1}\overline{\boldsymbol{ss}}\operatorname{diag}\{\boldsymbol{\varepsilon}\}\,. \tag{15}$$

It can be shown that $\overline{\boldsymbol{SS}}$ also obeys a reciprocity relation $\overline{S_i S_j} = \overline{S_j S_i}$ or equivalently $\overline{\boldsymbol{SS}} = \overline{\boldsymbol{SS}}^{\mathsf{T}}$. To be consistent with the energy balance, both $\overline{\boldsymbol{ss}}$ and $\overline{\boldsymbol{SS}}$ must satisfy some algebraic constraints known as *summation rules*. The radiation system acquires a state of *thermal equilibrium* if all surface temperatures become equal, leading to $\boldsymbol{E} = \sigma T^4 \mathbf{1}$ with the common temperature T. $\mathbf{1}$ represents a vector of unity components only. Thermal equilibrium requires $\boldsymbol{Q} = \mathbf{0}$. The specialization of (13b) and (13c) for the state of thermal equilibrium shows that $\boldsymbol{B} = \boldsymbol{H} = \boldsymbol{E}$. Insertion into (13a) and (14) yields the summation rules

$$\boldsymbol{S} = \overline{\boldsymbol{ss}}\mathbf{1}, \qquad \operatorname{diag}\{\boldsymbol{S}\}\,\boldsymbol{\varepsilon} = \overline{\boldsymbol{SS}}\mathbf{1}. \tag{16}$$

They can be helpful for checking numeric results of exchange areas or to reduce the workload for computing the exchange areas. This may be particularly interesting if approximate techniques like the Monte-Carlo method (cf. [20, 27, 38]) are employed for finding the exchange areas. However, in this analysis, the direct and total exchange areas are computed by means of (12) and (15), respectively.

4.3. Results for the furnace system

The findings of the previous section are now applied to the enclosures made up of the bottom and the top half of the furnace. Slabs which are currently reheated in the furnace have the bottom and top surface areas $\boldsymbol{S}^{\mp} = [S^{\mp}_{j_{start}}, S^{\mp}_{j_{start}+1}, \ldots, S^{\mp}_{j_{end}}]^{\mathsf{T}}$ and the corresponding emissivities $\boldsymbol{\varepsilon}^{\mp} = [\varepsilon^{\mp}_{j_{start}}, \varepsilon^{\mp}_{j_{start}+1}, \ldots, \varepsilon^{\mp}_{j_{end}}]^{\mathsf{T}}$.

Post-print version of the article: A. Steinboeck, D. Wild, T. Kiefer, and A. Kugi, "A mathematical model of a slab reheating furnace with radiative heat transfer and non-participating gaseous media", *International Journal of Heat and Mass Transfer*, vol. 53, no. 25-26, pp. 5933–5946, 2010. DOI: 10.1016/j.ijheatmasstransfer.2010.07.029
The content of this post-print version is identical to the published paper but without the publisher's final layout or copy editing.

As shown in Figure 1, the furnace volume is separated into N_z^- zones in the bottom half and N_z^+ zones in the top half with the homogeneously distributed zone temperatures $\boldsymbol{T}_z^{\mp} = [T_{z,1}^{\mp}, T_{z,2}^{\mp}, \ldots, T_{z,N_z^{\mp}}^{\mp}]^{\mathsf{T}}$. They serve as inputs of the model. The state vectors of all slabs in the furnace are summarized in the vector $\boldsymbol{x}(t) = [\boldsymbol{x}_{j_{start}}^{\mathsf{T}}(t), \boldsymbol{x}_{j_{start}+1}^{\mathsf{T}}(t), \ldots, \boldsymbol{x}_{j_{end}}^{\mathsf{T}}(t)]^{\mathsf{T}}$, which generally changes its size $3N_s$ with time. Utilizing the results of the Galerkin discretization from Section 3.3, the surface temperatures of the slabs follow as $\boldsymbol{M}^{\mp}\boldsymbol{x}(t)$ with the $N_s \times 3N_s$ sparse matrix $\boldsymbol{M}^{\mp} = \left[\delta_{i,j}\left[1 \quad \mp 1 \quad {}^2\!/_3\right]\right]_{i=1\ldots N_s, j=1\ldots N_s}$. Here, $\delta_{i,j}$ is the Kronecker delta. Therefore, the temperatures of all participating surfaces can be assembled as a vector $[(\boldsymbol{T}_z^{\mp})^{\mathsf{T}}, (\boldsymbol{M}^{\mp}\boldsymbol{x}(t))^{\mathsf{T}}]^{\mathsf{T}}$ and the corresponding total exchange area matrix $\overline{\boldsymbol{SS}}^{\mp}$ can be computed according to (15) for both the bottom and the top furnace half. Eventually, this allows the calculation of the net heat flux densities into the slabs as

$$\boldsymbol{q}^{\mp}(t) = \begin{bmatrix} q_{j_{start}}^{\mp}(t) & q_{j_{start}+1}^{\mp}(t) & \cdots & q_{j_{end}}^{\mp}(t) \end{bmatrix}^{\mathsf{T}} = \boldsymbol{P}_z^{\mp}\left(\boldsymbol{T}_z^{\mp}\right)^4 + \boldsymbol{P}_s^{\mp}\left(\boldsymbol{M}^{\mp}\boldsymbol{x}(t)\right)^4 \tag{17a}$$

with

$$\boldsymbol{P}_z^{\mp} = \left[P_{z,i,j}^{\mp}\right]_{\substack{i=j_{start}\cdots j_{end}\\ j=1\ldots N_z^{\mp}}} = \sigma\,\mathrm{diag}\left\{\boldsymbol{S}^{\mp}\right\}^{-1}\left[\boldsymbol{0}_{N_s\times N_z^{\mp}} \quad \boldsymbol{I}_{N_s\times N_s}\right]\overline{\boldsymbol{SS}}^{\mp}\begin{bmatrix}\boldsymbol{I}_{N_z^{\mp}\times N_z^{\mp}}\\ \boldsymbol{0}_{N_s\times N_z^{\mp}}\end{bmatrix} \tag{17b}$$

$$\boldsymbol{P}_s^{\mp} = \left[P_{s,i,j}^{\mp}\right]_{\substack{i=j_{start}\cdots j_{end}\\ j=j_{start}\cdots j_{end}}} = \sigma\,\mathrm{diag}\left\{\boldsymbol{S}^{\mp}\right\}^{-1}\left[\boldsymbol{0}_{N_s\times N_z^{\mp}} \quad \boldsymbol{I}_{N_s\times N_s}\right]\overline{\boldsymbol{SS}}^{\mp}\begin{bmatrix}\boldsymbol{0}_{N_z^{\mp}\times N_s}\\ \boldsymbol{I}_{N_s\times N_s}\end{bmatrix} - \sigma\,\mathrm{diag}\left\{\boldsymbol{\varepsilon}^{\mp}\right\}. \tag{17c}$$

The 4th power in (17a) is applied to each component of the respective vector. Equation (17) constitutes a radiation boundary condition which couples the dynamic systems of the slabs in the furnace. Throughout this paper, it is assumed that slabs are either fully inside or fully outside the furnace. If this were not the case, the concerned value $q_j^{\mp}(t)$ from (17a) would have to be scaled by the ratio between the total slab surface area $S_j^{\mp}$ and its portion that is participating in the radiative heat exchange process before it is inserted into (7) or (10).

Since, the slabs change their position, both $\boldsymbol{P}_z^{\mp}$ and $\boldsymbol{P}_s^{\mp}$ depend on t. Moreover, they are independent of the absolute size of the furnace, i. e., just the shape and the relative size of the participating surfaces play a role. The section is concluded with some remarks on the properties of (17), which highlight that the above results are in line with the *second law of thermodynamics*.

It is assumed that both $\boldsymbol{P}_z^{\mp}$ and $\boldsymbol{P}_s^{\mp}$ have at least one non-zero element in each row. Otherwise, the heat input into the respective slab would be independent of the surface temperatures $\boldsymbol{T}_z^{\mp}$ or $\boldsymbol{M}^{\mp}\boldsymbol{x}(t)$, respectively. This is only possible for special cases like $\varepsilon_j = 0$, which are ruled out in this analysis. In practice, $\boldsymbol{P}_z^{\mp}$ and $\boldsymbol{P}_s^{\mp}$ do not have any zero entries because there is radiative interaction between all surfaces

Post-print version of the article: A. Steinboeck, D. Wild, T. Kiefer, and A. Kugi, "A mathematical model of a slab reheating furnace with radiative heat transfer and non-participating gaseous media", *International Journal of Heat and Mass Transfer*, vol. 53, no. 25-26, pp. 5933–5946, 2010. DOI: 10.1016/j.ijheatmasstransfer.2010.07.029
The content of this post-print version is identical to the published paper but without the publisher's final layout or copy editing.

of an enclosure—at least through reflection. At any time, the components of $\boldsymbol{P}_z^{\mp}$ and $\boldsymbol{P}_s^{\mp}$ satisfy

$$0 \leq P_{z,i,j}^{\mp} < \sigma, \qquad |P_{s,i,j}^{\mp}| < \sigma, \tag{18a}$$

$$P_{s,i,j}^{\mp} \begin{cases} \geq 0 & \text{if } i \neq j \\ < 0 & \text{else} \end{cases}, \qquad \sum_{j=j_{start}}^{j_{end}} P_{s,i,j}^{\mp} < 0, \tag{18b}$$

$$\sum_{j=1}^{N_z^{\mp}} P_{z,i,j}^{\mp} + \sum_{j=j_{start}}^{j_{end}} P_{s,i,j}^{\mp} = 0. \tag{18c}$$

From (18b) and the Gershgorin circle theorem [11], it can be deduced that $\boldsymbol{P}_s^{\mp}$ is a Hurwitz matrix. (18c) follows directly from (16). (18) confirms that

- $q_j^{\mp}$ $\forall\, j \in J$ is monotonically *non-decreasing* with $[1 \quad \mp 1 \quad {}^2\!/_3]\, \boldsymbol{x}_i$ $\forall\, i \in J,\, i \neq j$,
- $q_j^{\mp}$ $\forall\, j \in J$ is monotonically *non-rising* with $[1 \quad \mp 1 \quad {}^2\!/_3]\, \boldsymbol{x}_j$, and
- $q_j^{\mp}$ $\forall\, j \in J$ is monotonically *non-decreasing* with $T_{z,i}^{\mp}$ $\forall\, i \in \{1, 2, \ldots, N_z^{\mp}\}$.

Furthermore, (18) confirms that for any $j \in J$ and for any t,

$$\begin{aligned} q_j^{\mp}(t) = 0 \quad \Rightarrow \quad & \min\left\{\{T_{z,1}^{\mp}, T_{z,2}^{\mp}, \ldots, T_{z,N_z^{\mp}}^{\mp}\} \cup \{[1 \quad \mp 1 \quad {}^2\!/_3]\, \boldsymbol{x}_i | i \in J, i \neq j\}\right\} \leq \\ & [1 \quad \mp 1 \quad {}^2\!/_3]\, \boldsymbol{x}_j(t) \leq \max\left\{\{T_{z,1}^{\mp}, T_{z,2}^{\mp}, \ldots, T_{z,N_z^{\mp}}^{\mp}\} \cup \{[1 \quad \mp 1 \quad {}^2\!/_3]\, \boldsymbol{x}_i | i \in J, i \neq j\}\right\}. \end{aligned} \tag{19}$$

These remarks may be useful for translating temperature bounds into constraints of the heat flux densities, or vice versa. They simplify the determination of extremal values. For instance, the considerations leading to (19) show that for the model inputs $\boldsymbol{T}_z^{\mp}$ being held at some constant value, the steady state solution requires that all slab temperatures are within the minimum and the maximum of $\boldsymbol{T}_z^{\mp}$.

5. Assembled dynamic system

The results of the previous sections are combined to obtain a dynamic system describing the furnace.

5.1. Continuous-time system

Specializing (7) and (8) for each slab inside the furnace and utilizing (17) yield the continuous-time system

$$\dot{\boldsymbol{x}}(t) = \boldsymbol{A}\boldsymbol{x}(t) + \boldsymbol{B}^{-}\left(\boldsymbol{P}_z^{-}\left(\boldsymbol{T}_z^{-}\right)^4 + \boldsymbol{P}_s^{-}\left(\boldsymbol{M}^{-}\boldsymbol{x}(t)\right)^4\right) + \boldsymbol{B}^{+}\left(\boldsymbol{P}_z^{+}\left(\boldsymbol{T}_z^{+}\right)^4 + \boldsymbol{P}_s^{+}\left(\boldsymbol{M}^{+}\boldsymbol{x}(t)\right)^4\right) \tag{20a}$$

with the sparse matrices

$$\boldsymbol{A} = \left[\delta_{i,j}\boldsymbol{a}_j\right]_{i=j_{start}\cdots j_{end}, j=j_{start}\cdots j_{end}}, \qquad \boldsymbol{B}^{\mp} = \left[\delta_{i,j}\boldsymbol{b}_j^{\mp}\right]_{i=j_{start}\cdots j_{end}, j=j_{start}\cdots j_{end}}. \tag{20b}$$

They depend on both $\boldsymbol{x}(t)$ (cf. (7b) and (8)) and t. Recall, that $\boldsymbol{P}_z^{\mp}$ and $\boldsymbol{P}_s^{\mp}$ also depend on t. The system (20) is locally *Lipschitz* in $\boldsymbol{x}(t)$ and piecewise continuous in t. Discontinuities may occur at $t = t_l^s$, i. e., when slabs are moved. Therefore, existence and uniqueness of the solution of (20) is ensured.

Post-print version of the article: A. Steinboeck, D. Wild, T. Kiefer, and A. Kugi, "A mathematical model of a slab reheating furnace with radiative heat transfer and non-participating gaseous media", *International Journal of Heat and Mass Transfer*, vol. 53, no. 25-26, pp. 5933–5946, 2010. DOI: 10.1016/j.ijheatmasstransfer.2010.07.029
The content of this post-print version is identical to the published paper but without the publisher's final layout or copy editing.

For slabs $j \notin J$, i. e., slabs that are currently outside the furnace, some other thermodynamic model or $q_j^{\mp}(t) = 0$ or $\dot{\boldsymbol{x}}_j(t) = \boldsymbol{0}$ may be used. The latter option is chosen in this analysis. Using the input transformation $\boldsymbol{u} = ([(\boldsymbol{T}_z^-)^\mathsf{T}, (\boldsymbol{T}_z^+)^\mathsf{T}]^\mathsf{T})^4$ shows that (20) constitutes an *input affine* system, which may be beneficial for controller design or dynamic optimization.

5.2. Discrete-time system

By analogy to the continuous-time case, the combination of (10) and (17) yields

$$\begin{aligned}\boldsymbol{x}_{k+1} = \boldsymbol{A}_k\boldsymbol{x}_k &+ \boldsymbol{B}_k^{1-}\left(\boldsymbol{P}_{z,k}^-\left(\boldsymbol{T}_z^-(t_k)\right)^4 + \boldsymbol{P}_{s,k}^-\left(\boldsymbol{M}^-\boldsymbol{x}_k\right)^4\right) + \boldsymbol{B}_k^{1+}\left(\boldsymbol{P}_{z,k}^+\left(\boldsymbol{T}_z^+(t_k)\right)^4 + \boldsymbol{P}_{s,k}^+\left(\boldsymbol{M}^+\boldsymbol{x}_k\right)^4\right)\\ &+ \boldsymbol{B}_k^{2-}\left(\boldsymbol{P}_{z,k}^-\left(\boldsymbol{T}_z^-(t_{k+1})\right)^4 + \boldsymbol{P}_{s,k}^-\left(\boldsymbol{M}^-\boldsymbol{x}_{k+1}\right)^4\right) + \boldsymbol{B}_k^{2+}\left(\boldsymbol{P}_{z,k}^+\left(\boldsymbol{T}_z^+(t_{k+1})\right)^4 + \boldsymbol{P}_{s,k}^+\left(\boldsymbol{M}^+\boldsymbol{x}_{k+1}\right)^4\right)\end{aligned} \tag{21}$$

with

$$\boldsymbol{x}_k = \begin{bmatrix}\boldsymbol{x}_{j_{start},k}^\mathsf{T} & \boldsymbol{x}_{j_{start}+1,k}^\mathsf{T} & \cdots & \boldsymbol{x}_{j_{end},k}^\mathsf{T}\end{bmatrix}^\mathsf{T}, \qquad \boldsymbol{P}_{z,k}^{\mp} = \lim_{\tau\to 0^+} \boldsymbol{P}_z^{\mp}\big|_{t=t_k+\tau}, \qquad \boldsymbol{P}_{s,k}^{\mp} = \lim_{\tau\to 0^+} \boldsymbol{P}_s^{\mp}\big|_{t=t_k+\tau}.$$

Similar to (20b), $\boldsymbol{A}_k$, $\boldsymbol{B}_k^{1\mp}$, and $\boldsymbol{B}_k^{2\mp}$ are the assemblies of $\boldsymbol{a}_{j,k}$, $\boldsymbol{b}_{j,k}^{1\mp}$, and $\boldsymbol{b}_{j,k}^{2\mp}$ from (10), respectively. It is emphasized that the piecewise linear shape of $\boldsymbol{q}^{\mp}(t)$ is a basic assumption of this approach. Therefore, the radiation boundary conditions defined by (17) are generally only satisfied at the sampling points t_k but not at times $t \in (t_k, t_{k+1})$. By analogy to the stipulations for the continuous-time case given in Section 5.1, the trivial mapping $\boldsymbol{x}_{j,k+1} = \boldsymbol{x}_{j,k}$ is used for slabs $j \notin J$, i. e., slabs that are currently outside the furnace.

The difference equation (21) can be numerically solved for $\boldsymbol{x}_{k+1}$, e. g., by means of the *Newton-Raphson* method, which exhibits *quadratic* convergence. When searching for $\boldsymbol{x}_{k+1}$, $\boldsymbol{x}_k$ proved to be a good starting point. Convergence problems have not been observed, even for coarse discretization of the time domain. The fact that (21) is an *implicit* equation is beneficial for the numeric stability of the integration method.

6. Stability analysis

It is assumed that the state space model (20) describes the real furnace accurately enough to transfer results of the stability analysis to the real system. It was observed in Section 4 that the radiative heat transfer model conforms to the second law of thermodynamics. At first glance, by virtue of this law, a stability analysis of the real system with the chosen inputs $\boldsymbol{T}_z^{\mp}$ seems dispensable. Indeed, the system cannot become unstable as long as zone temperatures $\boldsymbol{T}_z^{\mp}$ serve as system inputs rather than air and fuel supply rates, which are integrated in the system. This is a fundamental rationale for selecting $\boldsymbol{T}_z^{\mp}$ as inputs of the proposed model.

For linear dynamical systems, the dynamics of the open-loop control error equals that of the system itself, and the dynamic behavior is invariant with respect to shifts in the state space. Hence, the suitability of a linear system for open-loop control can be inferred from its stability properties. Generally, nonlinear systems like (20) do not exhibit these favorable features and, consequently, require a separate proof of stability of the dynamics of the open-loop control error and a definition of the region of convergence.

Post-print version of the article: A. Steinboeck, D. Wild, T. Kiefer, and A. Kugi, "A mathematical model of a slab reheating furnace with radiative heat transfer and non-participating gaseous media", *International Journal of Heat and Mass Transfer*, vol. 53, no. 25-26, pp. 5933–5946, 2010. DOI: 10.1016/j.ijheatmasstransfer.2010.07.029
The content of this post-print version is identical to the published paper but without the publisher's final layout or copy editing.

Therefore, the motivation of the following stability analysis is not to repeat what seems obvious according to the second law of thermodynamics, but to investigate the mathematical model in terms of its open-loop control error. Conditions will be derived, which ensure that some initial control error decreases exponentially. Under these conditions, open-loop operation of the furnace system is at least justified, although the dynamic behavior of the controlled system may be significantly improved if feedback is introduced. In fact, the reference [34] points out some drawbacks entailed by the absence of feedback control, especially if the controlled furnace system exhibits appreciable uncertainties.

To simplify the analysis, $\bar{c}_j$ and $\bar{\lambda}_j$ from (8) are assumed to be constant throughout this section. Before the complete furnace model is evaluated, the principle of the stability analysis is demonstrated for a single slab.

6.1. A single slab

Consider that there is only a single slab j whereas all other surface temperatures in the furnace—including the surface temperatures of other slabs defined by their states—serve as inputs of the dynamic system of slab j. Fortunately, the dynamic system follows directly by extracting the relevant rows of (20), i. e.,

$$\begin{aligned}\dot{\boldsymbol{x}}_j(t) = \boldsymbol{a}_j\boldsymbol{x}_j(t) + \boldsymbol{b}_j^- P_{s,j,j}^- \left([1 \quad -1 \quad 2/3]\,\boldsymbol{x}_j(t)\right)^4 + \boldsymbol{b}_j^+ P_{s,j,j}^+ \left([1 \quad 1 \quad 2/3]\,\boldsymbol{x}_j(t)\right)^4 \\ + \boldsymbol{u}_j(t, \boldsymbol{T}_z^-, \boldsymbol{T}_z^+, \boldsymbol{x}_{j_{start}}, \ldots, \boldsymbol{x}_{j-1}, \boldsymbol{x}_{j+1}, \ldots, \boldsymbol{x}_{j_{end}})\end{aligned} \tag{22}$$

with some input function $\boldsymbol{u}_j$ emerging from an appropriate decomposition of the matrices $\boldsymbol{B}^{\mp}\boldsymbol{P}_z^{\mp}$, $\boldsymbol{B}^{\mp}\boldsymbol{P}_s^{\mp}$, and $\boldsymbol{M}^{\mp}$.

Let $\tilde{\boldsymbol{x}}_j(t)$ be a reference trajectory which obeys (22) with the corresponding set of *reference inputs* $\tilde{\boldsymbol{T}}_z^-$, $\tilde{\boldsymbol{T}}_z^+$, $\tilde{\boldsymbol{x}}_{j_{start}}$, ... , $\tilde{\boldsymbol{x}}_{j-1}$, $\tilde{\boldsymbol{x}}_{j+1}$, ... , $\tilde{\boldsymbol{x}}_{j_{end}}$. For instance, this reference solution may have been found by dynamic optimization or it may be a steady state solution. Consider that the initial conditions $\boldsymbol{x}_{j,0}$ and $\tilde{\boldsymbol{x}}_{j,0}$ of the original system and of the reference solution, respectively, deviate from each other. Open-loop control by applying the above *reference inputs* is justified if the *error* $\boldsymbol{x}_j - \tilde{\boldsymbol{x}}_j$ in some sense decreases with t, which can be shown by analyzing the error dynamics of (22). To simplify the analysis, the regular coordinate transformation

$$\boldsymbol{z}_j = \boldsymbol{V}\boldsymbol{x}_j, \qquad \boldsymbol{V} = \begin{bmatrix} 1 & 0 & 0 \\ 1 & -1 & 2/3 \\ 1 & 1 & 2/3 \end{bmatrix} \tag{23}$$

is introduced. Since, the components of $\boldsymbol{z}_j$ represent the mean temperature and the surface temperatures of the slab, the reasonable restriction $\boldsymbol{z}_j \in D = \{\boldsymbol{v} \in \mathbb{R}^3 | \boldsymbol{v} > \delta\boldsymbol{1}\}$ with some small $\delta > 0$ will be used throughout the paper. Here, $\boldsymbol{v} > \delta\boldsymbol{1}$ means that the inequality relation holds true for all corresponding components of $\boldsymbol{v}$ and $\delta\boldsymbol{1}$, i. e., each component of $\boldsymbol{v}$ exceeds δ. Transforming the reference solution $\tilde{\boldsymbol{x}}_j(t)$ in the same manner, i. e., $\tilde{\boldsymbol{z}}_j = \boldsymbol{V}\tilde{\boldsymbol{x}}_j \in D$, and introducing the error $\boldsymbol{e}_j = \boldsymbol{z}_j - \tilde{\boldsymbol{z}}_j > \delta\boldsymbol{1} - \tilde{\boldsymbol{z}}_j$ yield the error dynamics

$$\dot{\boldsymbol{e}}_j(t) = \tilde{\boldsymbol{a}}_j\boldsymbol{e}_j(t) + \left(\tilde{\boldsymbol{b}}_j^- P_{s,j,j}^- [0 \quad 1 \quad 0] + \tilde{\boldsymbol{b}}_j^+ P_{s,j,j}^+ [0 \quad 0 \quad 1]\right)\left(\left(\boldsymbol{e}_j(t) + \tilde{\boldsymbol{z}}_j(t)\right)^4 - \left(\tilde{\boldsymbol{z}}_j(t)\right)^4\right) \tag{24a}$$

Post-print version of the article: A. Steinboeck, D. Wild, T. Kiefer, and A. Kugi, "A mathematical model of a slab reheating furnace with radiative heat transfer and non-participating gaseous media", *International Journal of Heat and Mass Transfer*, vol. 53, no. 25-26, pp. 5933–5946, 2010. DOI: 10.1016/j.ijheatmasstransfer.2010.07.029
The content of this post-print version is identical to the published paper but without the publisher's final layout or copy editing.

with

$$\tilde{\boldsymbol{a}}_j = -\frac{12\bar{\lambda}_j}{\rho_j \bar{c}_j D_j^2}\begin{bmatrix} 0 & 0 & 0 \\ -5 & 3 & 2 \\ -5 & 2 & 3 \end{bmatrix}, \qquad \tilde{\boldsymbol{b}}_j^{\mp} = \frac{1}{\rho_j \bar{c}_j D_j}\begin{bmatrix} 1 \\ 6 \pm 3 \\ 6 \mp 3 \end{bmatrix}. \tag{24b}$$

Using the positive definite Lyapunov function candidate

$$w(\boldsymbol{e}_j) = \frac{30}{D_j}\int_{-D_j/2}^{D_j/2} \left(\begin{bmatrix} h_{j,1}(y) & h_{j,2}(y) & h_{j,3}(y) \end{bmatrix} \boldsymbol{V}^{-1}\boldsymbol{e}_j\right)^2 \mathrm{d}y = \boldsymbol{e}_j^{\mathsf{T}}\boldsymbol{p}\boldsymbol{e}_j, \qquad \boldsymbol{p} = \begin{bmatrix} 36 & -3 & -3 \\ -3 & 4 & -1 \\ -3 & -1 & 4 \end{bmatrix},$$

it follows that

$$\dot{w}(\boldsymbol{e}_j) = \boldsymbol{e}_j^{\mathsf{T}}\left(\boldsymbol{p}\tilde{\boldsymbol{a}}_j + \tilde{\boldsymbol{a}}_j^{\mathsf{T}}\boldsymbol{p}\right)\boldsymbol{e}_j + \boldsymbol{e}_j^{\mathsf{T}}\frac{60}{\rho_j \bar{c}_j D_j}\operatorname{diag}\begin{Bmatrix} 0 & P_{s,j,j}^{-} & P_{s,j,j}^{+} \end{Bmatrix}\left(\left(\boldsymbol{e}_j + \tilde{\boldsymbol{z}}_j\right)^4 - \tilde{\boldsymbol{z}}_j^4\right)$$

with negative semidefinite

$$\boldsymbol{p}\tilde{\boldsymbol{a}}_j + \tilde{\boldsymbol{a}}_j^{\mathsf{T}}\boldsymbol{p} = -\frac{120\bar{\lambda}_j}{\rho_j \bar{c}_j D_j^2}\begin{bmatrix} 6 & -3 & -3 \\ -3 & 2 & 1 \\ -3 & 1 & 2 \end{bmatrix}.$$

Because of $\boldsymbol{e}_j^{\mathsf{T}}((\boldsymbol{e}_j + \tilde{\boldsymbol{z}}_j)^4 - \tilde{\boldsymbol{z}}_j^4) \geq \delta^3 \boldsymbol{e}_j^{\mathsf{T}}\boldsymbol{e}_j$ for $\boldsymbol{e}_j > \delta\mathbf{1} - \tilde{\boldsymbol{z}}_j$ and $\tilde{\boldsymbol{z}}_j \in D$ and since there exists a suitable constant $\bar{P}_j$ such that $P_{s,j,j}^{\mp} < \bar{P}_j < 0$ (cf. (18b)),

$$\dot{w}(\boldsymbol{e}_j) \leq \bar{w}(\boldsymbol{e}_j) = \boldsymbol{e}_j^{\mathsf{T}}\left(\boldsymbol{p}\tilde{\boldsymbol{a}}_j + \tilde{\boldsymbol{a}}_j^{\mathsf{T}}\boldsymbol{p} + \frac{60\delta^3\bar{P}_j}{\rho_j \bar{c}_j D_j}\operatorname{diag}\begin{Bmatrix} 0 & 1 & 1 \end{Bmatrix}\right)\boldsymbol{e}_j$$

with negative definite $\bar{w}(\boldsymbol{e}_j)$. The above results require that the slab j is inside the furnace—otherwise, $\dot{\boldsymbol{e}}_j(t) = \mathbf{0}$ and $\dot{w}(\boldsymbol{e}_j) = 0$.

Hence, according to *Lyapunov's direct method* [21, 39], the equilibrium $\boldsymbol{e}_j(t) = \mathbf{0}\ \forall\ t$ of (24) is *uniformly stable*. Moreover, it is even *exponentially stable* if the slab j is always inside the furnace. These results do not hold globally, since $\boldsymbol{e}_j > \delta\mathbf{1} - \tilde{\boldsymbol{z}}_j$ and $\tilde{\boldsymbol{z}}_j \in D$. However, this is just a weak restriction because temperature ranges below δ are practically irrelevant. Consequently, it is *safe* to operate the system (22) with open-loop control if $\bar{c}_j$ and $\bar{\lambda}_j$ are constant and if $\boldsymbol{z}_j(t)$, $\tilde{\boldsymbol{z}}_j(t) \in D$.

6.2. The furnace system with immobile slabs

Assuming that the slabs do not move, sufficient conditions for exponential stability of the system (20) will be given. Therefore, $\boldsymbol{A}$, $\boldsymbol{B}$, $\boldsymbol{P}_z^{\mp}$, and $\boldsymbol{P}_s^{\mp}$ are constant, and only slabs $j \in J$ inside the furnace are considered. Introduction of the equality constraints $\boldsymbol{S}^{-} = \boldsymbol{S}^{+}$, $\boldsymbol{P}_z^{-} = \boldsymbol{P}_z^{+}$, and $\boldsymbol{P}_s^{-} = \boldsymbol{P}_s^{+}$ requires that the shapes of the multi-surface enclosures formed by the bottom and the top half of the furnace are symmetric. Again, let $\tilde{\boldsymbol{x}}(t)$ be a reference trajectory which obeys (20) with the corresponding *reference inputs* $\tilde{\boldsymbol{T}}_z^{-}$ and $\tilde{\boldsymbol{T}}_z^{+}$, and consider that the initial conditions $\boldsymbol{x}_0$ and $\tilde{\boldsymbol{x}}_0$ deviate from each other.

To show that the *error* $\boldsymbol{x} - \tilde{\boldsymbol{x}}$ in some sense decreases with t, it is helpful to apply the transformation (23) to each slab. Let $\tilde{\boldsymbol{z}}(t)$ be the reference solution corresponding to the transformed state vector $\boldsymbol{z}(t)$. Also, the constraints $\boldsymbol{z}_j(t)$, $\tilde{\boldsymbol{z}}_j(t) \in D$ are used for each slab. Then, the dynamics of the error $\boldsymbol{e} = \boldsymbol{z} - \tilde{\boldsymbol{z}} > \delta\mathbf{1} - \tilde{\boldsymbol{z}}$

Post-print version of the article: A. Steinboeck, D. Wild, T. Kiefer, and A. Kugi, "A mathematical model of a slab reheating furnace with radiative heat transfer and non-participating gaseous media", *International Journal of Heat and Mass Transfer*, vol. 53, no. 25-26, pp. 5933–5946, 2010. DOI: 10.1016/j.ijheatmasstransfer.2010.07.029
The content of this post-print version is identical to the published paper but without the publisher's final layout or copy editing.

reads as

$$\dot{\boldsymbol{e}}(t) = \tilde{\boldsymbol{A}}\boldsymbol{e}(t) + \left(\tilde{\boldsymbol{B}}^{-}\boldsymbol{P}_s^{-}\tilde{\boldsymbol{M}}^{-} + \tilde{\boldsymbol{B}}^{+}\boldsymbol{P}_s^{+}\tilde{\boldsymbol{M}}^{+}\right)\left((\boldsymbol{e}(t) + \tilde{\boldsymbol{z}}(t))^4 - (\tilde{\boldsymbol{z}}(t))^4\right) \tag{25}$$

with the sparse matrices $\tilde{\boldsymbol{M}}^{-} = \left[\delta_{3i,j+1}\right]_{i=1\ldots N_s, j=1\ldots 3N_s}$ and $\tilde{\boldsymbol{M}}^{+} = \left[\delta_{3i,j}\right]_{i=1\ldots N_s, j=1\ldots 3N_s}$. By analogy to (20b), $\tilde{\boldsymbol{A}}$ and $\tilde{\boldsymbol{B}}^{\mp}$ are the assemblies of $\tilde{\boldsymbol{a}}_j$ and $\tilde{\boldsymbol{b}}_j^{\mp}$ from (24b), respectively. Using the positive definite Lyapunov function candidate $W(\boldsymbol{e}) = \boldsymbol{e}^{\mathsf{T}}\boldsymbol{P}\boldsymbol{e}$ with symmetric positive definite matrices

$$\boldsymbol{P} = \boldsymbol{P}^{\mathsf{T}} = \left[P_{i,j}\boldsymbol{p}\right]_{i=j_{start}\cdots j_{end}, j=j_{start}\cdots j_{end}}$$
$$\left[P_{i,j}\right]_{\substack{i=j_{start}\cdots j_{end}\\ j=j_{start}\cdots j_{end}}} = -\operatorname{diag}\left\{\left[\rho_j\bar{c}_jD_jS_j^{\mp}\right]_{j=j_{start}\cdots j_{end}}\right\}(\boldsymbol{P}_s^{\mp})^{-1}\operatorname{diag}\left\{\left[\rho_j\bar{c}_jD_j\right]_{j=j_{start}\cdots j_{end}}\right\},$$

it follows that

$$\dot{W}(\boldsymbol{e}) = \boldsymbol{e}^{\mathsf{T}}\left(\boldsymbol{P}\tilde{\boldsymbol{A}} + \tilde{\boldsymbol{A}}^{\mathsf{T}}\boldsymbol{P}\right)\boldsymbol{e} - \boldsymbol{e}^{\mathsf{T}}60\left[\delta_{i,j}\rho_j\bar{c}_jD_jS_j^{\mp}\operatorname{diag}\{0 \quad 1 \quad 1\}\right]_{i=j_{start}\cdots j_{end}, j=j_{start}\cdots j_{end}}\left((\boldsymbol{e}+\tilde{\boldsymbol{z}})^4 - \tilde{\boldsymbol{z}}^4\right)$$

and

$$\dot{W}(\boldsymbol{e}) \le \bar{W}(\boldsymbol{e}) = \boldsymbol{e}^{\mathsf{T}}\left(\boldsymbol{P}\tilde{\boldsymbol{A}} + \tilde{\boldsymbol{A}}^{\mathsf{T}}\boldsymbol{P} - \delta^3 240\left[\delta_{i,j}\rho_j\bar{c}_jD_jS_j^{\mp}\operatorname{diag}\{0 \quad 1 \quad 1\}\right]_{i=j_{start}\cdots j_{end}, j=j_{start}\cdots j_{end}}\right)\boldsymbol{e}.$$

Therefore, it remains to provide conditions for the symmetric matrix

$$\boldsymbol{P}\tilde{\boldsymbol{A}} + \tilde{\boldsymbol{A}}^{\mathsf{T}}\boldsymbol{P} = \left[P_{i,j}\left(\boldsymbol{p}\tilde{\boldsymbol{a}}_j + \tilde{\boldsymbol{a}}_i^{\mathsf{T}}\boldsymbol{p}\right)\right]_{\substack{i=j_{start}\cdots j_{end}\\ j=j_{start}\cdots j_{end}}} = -60\left[P_{i,j}(d_i+d_j)\begin{bmatrix}6 & -3 & -3\\ -3 & 2 & 1\\ -3 & 1 & 2\end{bmatrix}\right]_{\substack{i=j_{start}\cdots j_{end}\\ j=j_{start}\cdots j_{end}}}$$

with

$$d_j = \frac{\bar{\lambda}_j}{\rho_j\bar{c}_jD_j^2}$$

to be negative semidefinite. It can be shown that it is negative semidefinite if the symmetric matrix

$$\left[P_{i,j}(d_i+d_j)\right]_{i=j_{start}\cdots j_{end}, j=j_{start}\cdots j_{end}} \tag{26}$$

is positive definite. Pre- and postmultiplying (26) by

$$\boldsymbol{P}_s^{\mp\mathsf{T}}\operatorname{diag}\left\{\left[\rho_j\bar{c}_jD_j\right]_{j=j_{start}\cdots j_{end}}\right\}^{-1} \qquad \text{and} \qquad \operatorname{diag}\left\{\left[\rho_j\bar{c}_jD_j\right]_{j=j_{start}\cdots j_{end}}\right\}^{-1}\boldsymbol{P}_s^{\mp},$$

do not change its definiteness and yield the symmetric matrix $-\left[S_i^{\mp}P_{s,i,j}^{\mp}(d_i+d_j)\right]_{i=j_{start}\cdots j_{end}, j=j_{start}\cdots j_{end}}$. Utilizing the Gershgorin circle theorem [11], positive definiteness of the latter is ensured if

$$-2P_{s,i,i}^{\mp}d_i > \sum_{\substack{j=j_{start}\\ j\neq i}}^{j_{end}} P_{s,i,j}^{\mp}(d_i+d_j) \quad \forall\, i \in J. \tag{27a}$$

Post-print version of the article: A. Steinboeck, D. Wild, T. Kiefer, and A. Kugi, "A mathematical model of a slab reheating furnace with radiative heat transfer and non-participating gaseous media", *International Journal of Heat and Mass Transfer*, vol. 53, no. 25-26, pp. 5933–5946, 2010. DOI: 10.1016/j.ijheatmasstransfer.2010.07.029
The content of this post-print version is identical to the published paper but without the publisher's final layout or copy editing.

For practical computations, it may be more convenient to use the condition

$$1 > \frac{1}{2}\left(1 + \frac{\max\limits_{j\in J}\{d_j\}}{\min\limits_{j\in J}\{d_j\}}\right)\max_{i\in J}\left\{ - \sum_{\substack{j=j_{start}\\ j\neq i}}^{j_{end}} \frac{P^{\mp}_{s,i,j}}{P^{\mp}_{s,i,i}}\right\}, \tag{27b}$$

which is a conservative estimate of (27a). It follows from (18b) that the last factor of (27b) never exceeds unity. Hence, if the values of d_j do not vary too much, $\boldsymbol{P}\tilde{\boldsymbol{A}} + \tilde{\boldsymbol{A}}^{\mathsf{T}}\boldsymbol{P}$ is negative semidefinite. It is emphasized that the conditions (27) are sufficient but not necessary for negative definiteness of $\boldsymbol{P}\tilde{\boldsymbol{A}} + \tilde{\boldsymbol{A}}^{\mathsf{T}}\boldsymbol{P}$.

Lyapunov's direct method [21, 39] shows that the equilibrium $\boldsymbol{e}(t) = \boldsymbol{0}\ \forall\ t$ of (25) is *exponentially stable*. This result does not hold globally, since $\boldsymbol{e} > \delta\boldsymbol{1} - \tilde{\boldsymbol{z}}$ and $\tilde{\boldsymbol{z}}_j \in D\ \forall j \in J$. Consequently, it is *safe* to operate the system (20) with open-loop control if the slabs are not moved, if $\bar{c}_j$ and $\bar{\lambda}_j$ are constant, if $\boldsymbol{z}_j(t)$, $\tilde{\boldsymbol{z}}_j(t) \in D\ \forall j \in J$, if $\boldsymbol{S}^- = \boldsymbol{S}^+$, $\boldsymbol{P}^-_z = \boldsymbol{P}^+_z$, and $\boldsymbol{P}^-_s = \boldsymbol{P}^+_s$, and if (27a) holds.

Given some initial error $\boldsymbol{e}(t_0)$ at t_0, exponential stability of the system (25) ensures that

$$\|\boldsymbol{e}(t)\|_2^2 \leq \|\boldsymbol{e}(t_0)\|_2^2\,\frac{k_2}{k_1}\,\mathrm{e}^{-\frac{k_3}{k_2}(t-t_0)} \quad \forall\ t \geq t_0 \tag{28}$$

(cf. [21, 39]) with

$$\begin{aligned} k_1 &= \mu_{\min}(\boldsymbol{P}), \qquad k_2 = \mu_{\max}(\boldsymbol{P}),\\ k_3 &= \mu_{\min}\Big(- \boldsymbol{P}\tilde{\boldsymbol{A}} - \tilde{\boldsymbol{A}}^{\mathsf{T}}\boldsymbol{P} + \delta^3 240\left[\delta_{i,j}\rho_j\bar{c}_j D_j S_j^{\mp}\,\mathrm{diag}\,\{0 \quad 1 \quad 1\}\right]_{i=j_{start}\cdots j_{end}, j=j_{start}\cdots j_{end}}\Big), \end{aligned}$$

where $\mu_{\min}(\cdot)$ and $\mu_{\max}(\cdot)$ are the minimum and maximum eigenvalue of the respective matrix. Hence, the period

$$\Delta t_{\min} = \frac{k_2}{k_3}\ln\left(\frac{k_2}{k_1}\right) \tag{29a}$$

is sufficient to ensure

$$\|\boldsymbol{e}(t)\|_2^2 \leq \|\boldsymbol{e}(t_0)\|_2^2 \quad \forall\ t \geq t_0 + \Delta t_{\min}. \tag{29b}$$

6.3. The furnace system with moving slabs

In contrast to the assumption of the previous section, slabs recurrently change their position. Once, a slab j has left the furnace, the proposed model defines $\dot{\boldsymbol{x}}_j(t) = \boldsymbol{0}$. Therefore, the system cannot be asymptotically stable, unless all considered slabs would remain in the furnace for ever—an unrealistic scenario.

If the real furnace operation is analyzed for an infinite period of time, the number of slabs grows without bounds. However, to simplify the following analysis, only N^s ($N_s \ll N^s < \infty$) slabs will be considered. The fact that N^s is a finite number is not a restriction because the slabs may repeatedly enter the furnace or the slab movement may be stopped sometimes in the distant future.

Like in the previous sections, let $\tilde{\boldsymbol{z}}_j(t)\ \forall\ j \in \{1, 2, \ldots, N^s\}$ be the reference solution corresponding to

Post-print version of the article: A. Steinboeck, D. Wild, T. Kiefer, and A. Kugi, "A mathematical model of a slab reheating furnace with radiative heat transfer and non-participating gaseous media", *International Journal of Heat and Mass Transfer*, vol. 53, no. 25-26, pp. 5933–5946, 2010. DOI: 10.1016/j.ijheatmasstransfer.2010.07.029
The content of this post-print version is identical to the published paper but without the publisher's final layout or copy editing.

$\tilde{\boldsymbol{T}}_z^-$ and $\tilde{\boldsymbol{T}}_z^+$. Then, the convergence of the error

$$\boldsymbol{e}^s(t) = \begin{bmatrix}\boldsymbol{e}_1^\mathsf{T}(t) & \boldsymbol{e}_2^\mathsf{T}(t) & \cdots & \boldsymbol{e}_{N^s}^\mathsf{T}(t)\end{bmatrix}^\mathsf{T}, \qquad \boldsymbol{e}_j = \boldsymbol{z}_j - \tilde{\boldsymbol{z}}_j \;\; \forall\, j \in \{1, 2, \ldots, N^s\}$$

towards the equilibrium $\boldsymbol{e}^s(t) = \boldsymbol{0}$ may be analyzed by means of the positive definite Lyapunov function candidate

$$W^s(\boldsymbol{e}^s) = \|\boldsymbol{e}^s\|_2^2.$$

Recall that the slabs are moved at the pushing times t_l^s, which refer to the sampling points of the discrete-time dynamical system of the error $\boldsymbol{e}^s$. Furthermore, consider $\Delta t_{\min,l}$ to be the minimum time period according to (29a) that is valid in the interval $[t_l^s, t_{l+1}^s)$. Therefore, if $t_{l+1}^s > t_l^s + \Delta t_{\min,l}$ $\forall\, l \in \mathbb{N}$, (29b) ensures

$$W^s(\boldsymbol{e}^s(t_{l+1}^s)) \leq W^s(\boldsymbol{e}^s(t_l^s)), \tag{30}$$

such that according to *Lyapunov's direct method* the discrete-time system with the series $(\boldsymbol{e}^s(t_l^s))$ is *uniformly stable* [39]. Note that the equality in (30) only holds if during the interval $[t_l^s, t_{l+1}^s)$ $\boldsymbol{e}_j(t) = \boldsymbol{0}$ $\forall\, j \in J$. Finally, the trajectory $\boldsymbol{e}^s(t)$ remains finite within each interval $[t_l^s, t_{l+1}^s)$ because of $\|\boldsymbol{e}(t_l^s)\|_2^2 \leq W^s(\boldsymbol{e}^s(t_l^s))$ and (28). Consequently, it is *safe* to operate the system (20) with open-loop control if $\boldsymbol{z}_j(t)$, $\tilde{\boldsymbol{z}}_j(t) \in D$ $\forall\, j \in \{1, 2, \ldots, N^s\}$ and if within each time interval $[t_l^s, t_{l+1}^s)$ the parameters $\bar{c}_j$ and $\bar{\lambda}_j$ are constant, $\boldsymbol{S}^- = \boldsymbol{S}^+$, $\boldsymbol{P}_z^- = \boldsymbol{P}_z^+$, and $\boldsymbol{P}_s^- = \boldsymbol{P}_s^+$, and (27a) holds.

7. Example problem

The slab temperature profile is an important output of the proposed model. Since the derived set of equations (cf. (20), (21)) contains only physical parameters which are (at least roughly) known, there is basically *no* need for parameter identification, and the model can be used *as is*. However, for verification purposes only, a measurement experiment was done on a pusher-type reheating furnace (cf. [40]) with $N_z^\mp = 5$ zones and the values were compared with results from the discrete-time model (21).

Admittedly, the accuracy of the mathematical model could be improved by identification of model parameters. In this case, sufficient measurement data would be required for both parameter estimation and verification. Note that only an independent data set—not exploited in the identification process—is suitable for verification. As discussed in [34], the need for multiple measurement series usually renders parameter identification for a furnace model a laborious and costly task. However, improving the accuracy can enhance the utility of the model and, hence, compensates for the additional effort during the implementation phase. Nevertheless, in this study, it was refrained from engaging with identification.

For the verification experiment, a 365 mm thick test slab j was equipped with a data acquisition unit enclosed by a water-cooled and insulated housing. Several thermocouples were assembled inside the slab at defined y-positions and connected to the data acquisition system. Hence, it was possible to record the complete temperature trajectory of the slab. Zone temperature values $\boldsymbol{T}_z^\mp$ were obtained from existing

Post-print version of the article: A. Steinboeck, D. Wild, T. Kiefer, and A. Kugi, "A mathematical model of a slab reheating furnace with radiative heat transfer and non-participating gaseous media", *International Journal of Heat and Mass Transfer*, vol. 53, no. 25-26, pp. 5933–5946, 2010. DOI: 10.1016/j.ijheatmasstransfer.2010.07.029
The content of this post-print version is identical to the published paper but without the publisher's final layout or copy editing.

thermocouples, which are located on the inner surface of the refractory furnace wall. The test slab entered

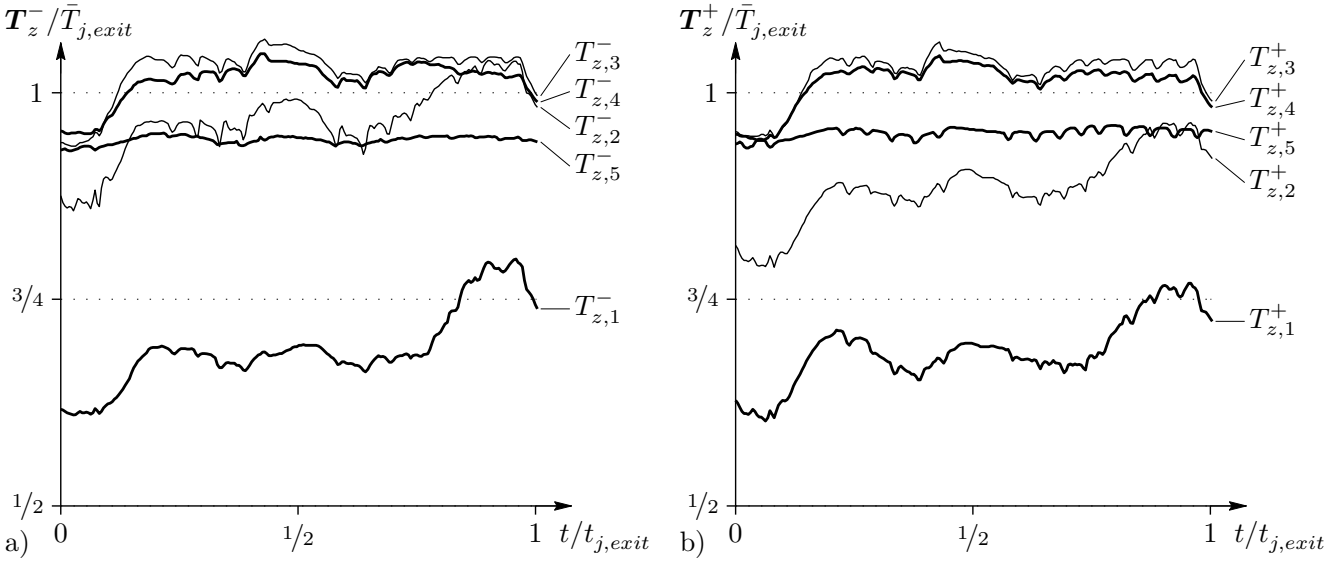

Figure 7: Measured zone temperatures, a) bottom half of the furnace, b) top half of the furnace.

the furnace at the time $t = 0$ and was withdrawn at $t = t_{j,exit}$. For this period, the measured zone temperatures are shown in Figure 7. The values served as inputs for the proposed simulation model (21). For clarity and comparability, all plots have been scaled such that both the period $[0, t_{j,exit}]$ and the range between the initial slab temperature $T_{j,0}$ and the mean value of the measured final slab temperature profile $\bar{T}_{j,exit}$ are mapped to the interval $[0, 1]$.

The corresponding temperature trajectory $T_j(y, t)$ of the instrumented slab is shown in Figure 8 for the positions $y = -0.3D_j$ and $y = 0$, i. e., for a near-surface region and the core of the slab. The simulation was executed with sampling periods $\Delta t_k < 2\,\text{min}$. Generally, Δt_k varies because sampling points t_k must occur at least at pushing times t_l^s. The results of (21) are compared to the measurement values and results of the elaborate simulation model presented in [40].

The computation time required by the reduced model is approximately 0.7 % of the time consumed by the model described in [40]. As demonstrated in [37], the computational effort can be further reduced without significant loss of accuracy if the sampling period Δt_k is increased. The results showed sufficient robustness against variations of Δt_k. In view of the intended purpose of the model, e. g., control and optimization, the achieved accuracy and the moderate computational costs are considered as an acceptable compromise.

8. Conclusion

A mathematically simple model of industrial slab reheating furnaces was developed and implemented for a pusher-type reheating furnace. However, the proposed method can be easily transferred to other slab reheating furnaces. The model allows the computation of a 1-dimensional approximation of the transient temperature field $T_j(y, t)$ of each slab, even if material parameters are significantly nonlinear. The dynamic subsystems of the slabs are coupled by radiation boundary conditions. Here, the zone temperatures $\boldsymbol{T}_z^{\mp}(t)$ serve as model inputs and play an important role for the radiative heat transfer in the slab reheating furnace.

Post-print version of the article: A. Steinboeck, D. Wild, T. Kiefer, and A. Kugi, “A mathematical model of a slab reheating furnace with radiative heat transfer and non-participating gaseous media”, *International Journal of Heat and Mass Transfer*, vol. 53, no. 25-26, pp. 5933–5946, 2010. DOI: 10.1016/j.ijheatmasstransfer.2010.07.029
The content of this post-print version is identical to the published paper but without the publisher’s final layout or copy editing.

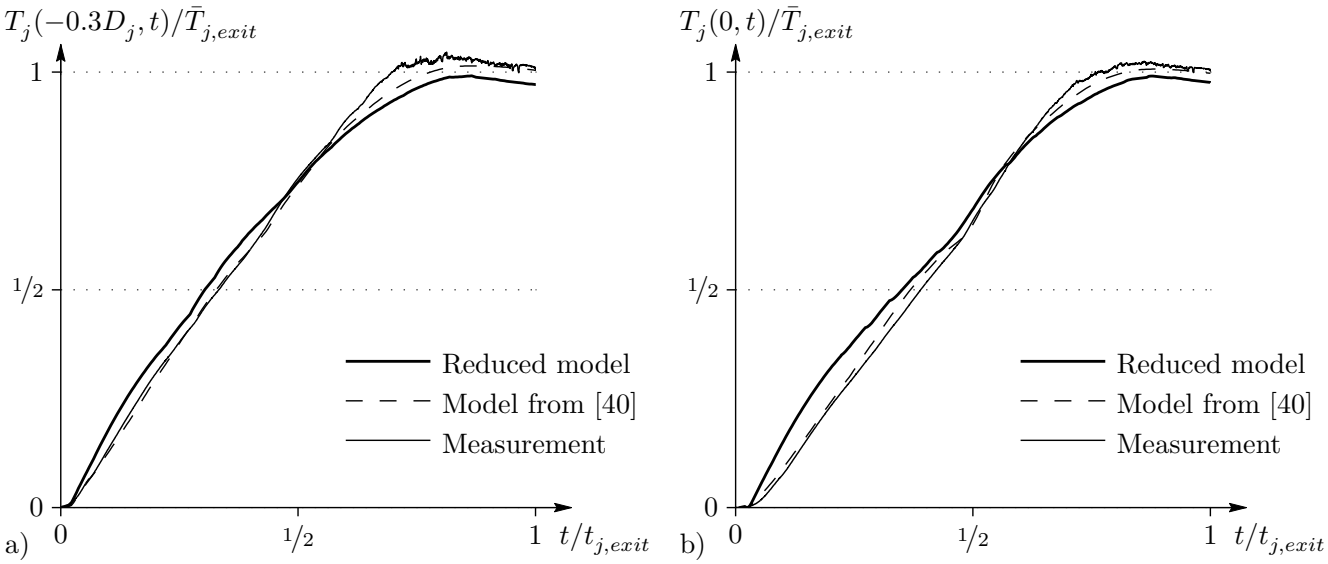

Figure 8: Trajectories of the slab temperature, a) for a near-surface region, b) for the core of the slab.

For a single slab with Neumann boundary conditions, the heat conduction problem (1) was solved by means of the Galerkin method with $H = 3$ trial functions (6). Based on the assumption of piecewise linear heat flux inputs (9) into the slab surfaces, the obtained ODE (7) and (8) was integrated yielding a discrete-time system (10). Here, the temperature dependence of the material parameters was approximately accounted for.

Next, the net radiation method was utilized for determining the heat flux densities (17) into the slabs as a function of the surface temperatures in the furnace. A number of assumptions concerning the geometry and the radiative behavior of the surfaces and the atmosphere in the furnace helped to keep the mathematical model as simple as possible. It was shown that the obtained results are in line with the second law of thermodynamics.

Some conditions were discussed which justify open-loop control of the system. Moreover, measurement results from an instrumented slab demonstrated the acceptable accuracy of the proposed method. Since all parameters of the model reflect physical quantities of the real system, laborious identification processes are effectively avoided.

The main advantages of the proposed mathematical model are acceptable accuracy combined with moderate computational costs, good convergence behavior, even for large sampling periods, sufficient consideration of temperature-dependent material parameters, and adequate incorporation of radiation boundary conditions. The benefit of the small model dimensions should become particularly apparent in real-time applications. Hence, the mathematical model may be adequate for implementation in supervisory process control, trajectory planning, optimization, or controller design for reheating furnaces.

Acknowledgments

The authors from Vienna University of Technology are much indebted to AG der Dillinger Hüttenwerke for its ongoing support as regards both subject matter and financing.

Post-print version of the article: A. Steinboeck, D. Wild, T. Kiefer, and A. Kugi, “A mathematical model of a slab reheating furnace with radiative heat transfer and non-participating gaseous media”, *International Journal of Heat and Mass Transfer*, vol. 53, no. 25-26, pp. 5933–5946, 2010. DOI: 10.1016/j.ijheatmasstransfer.2010.07.029
The content of this post-print version is identical to the published paper but without the publisher’s final layout or copy editing.

References

[1] H.D. Baehr and K. Stephan. *Heat and Mass Transfer*. Springer-Verlag, Berlin Heidelberg, 2nd edition, 2006.

[2] S. Banerjee, D. Sanyal, S. Sen, and I.K. Puri. A methodology to control direct-fired furnaces. *International Journal of Heat and Mass Transfer*, 47:5247–5256, 2004.

[3] P.V. Barr. The development, verification, and application of a steady-state thermal model for the pusher-type reheat furnace. *Metallurgical and Materials Transactions B*, 26B:851–869, August 1995.

[4] S. Chen, S. Abraham, and D. Poshard. Modification of reheat furnace practices through comprehensive process modeling. *Iron & Steel Technology*, 5(8):66–79, August 2008.

[5] G. van Ditzhuijzen, D. Staalman, and A. Koorn. Identification and model predictive control of a slab reheating furnace. *Proceedings of the 2002 IEEE International Conference on Control Applications, Glasgow, UK*, pages 361–366, September 2002.

[6] D.G. Elliston, W.A. Gray, D.F. Hibberd, T.Y. Ho, and A. Williams. The effects of surface emissivity on furnace performance. *Journal of the Institute of Energy*, 60:155–167, 1987.

[7] H. Ezure, Y. Seki, N. Yamaguchi, and H. Shinonaga. Development of a simulator to calculate an optimal slab heating pattern for reheat furnaces. *Electrical Engineering in Japan*, 120(3):42–53, 1997.

[8] C. Fletcher. *Computational Galerkin Methods*. Springer, New York, 1984.

[9] P. Fontana, A. Boggiano, A. Furinghetti, G. Cabras, and C.A. Simoncini. An advanced computer control system for reheat furnaces. *Iron and Steel Engineer*, 60(8):55–62, August 1983.

[10] G.F. Franklin, J.D. Powell, and M. Workman. *Digital Control of Dynamic Systems*. Prentice Hall, Upper Saddle River, NJ, 3rd edition, 1997.

[11] G.H. Golub and C.F. van Loan. *Matrix Computations*. Johns Hopkins Series in the Mathematical Sience. The Johns Hopkins University Press, Baltimore, London, 3rd edition, 1996.

[12] J.M. Goyhénèche and J.F. Sacadura. The zone method: A new explicit matrix relation to calculate the total exchange areas in anisotropically scattering medium bounded by anisotropically reflecting walls. *Journal of Heat Transfer*, 124(4):696–703, August 2002.

[13] S.H. Han, S.W. Baek, and M.Y. Kim. Transient radiative heating characteristics of slabs in a walking beam type reheating furnace. *International Journal of Heat and Mass Transfer*, 52:1005–1011, 2009.

[14] K. Harste. *Untersuchung zur Schrumpfung und zur Entstehung von mechanischen Spannungen während der Erstarrung und nachfolgender Abkühlung zylindrischer Blöcke aus Fe-C-Legierungen*. PhD thesis, Technische Universität Clausthal, 1989.

[15] F. Hollander and S.P.A. Zuurbier. Design, development and performance of online computer control in a 3-zone reheating furnace. *Iron and Steel Engineer*, 59(1):44–52, January 1982.

[16] M. Honner, Z. Vesely, and M. Svantner. Exodus stochastic method application in the continuous reheating furnace control system. *Scandinavian Journal of Metallurgy*, 33:328–337, 2004.

[17] H.C. Hottel and A.F. Sarofim. *Radiative Transfer*. McGraw-Hill, New York, 1967.

[18] Z.A. Icev, J. Zhao, M.J. Stankovski, T.D. Kolemisevska-Gugulovska, and G.M. Dimirovski. Supervisory-plus-regulatory control design for efficient operation of industrial furnaces. *Journal of Electrical & Electronics Engineering*, 4(2):1199–1218, 2004.

[19] F.P. Incropera, D.P. DeWitt, T.L. Bergman, and A.S. Lavine. *Fundamentals of Heat and Mass Transfer*. J. Wiley & Sons, Hoboken, NJ, 6th edition, 2007.

[20] A. Jaklič, F. Vode, and T. Kolenko. Online simulation model of the slab-reheating process in a pusher-type furnace. *Applied Thermal Engineering*, 27:1105–1114, 2007.

[21] H.K. Khalil. *Nonlinear Systems*. Prentice Hall, New Jersey, 3rd edition, 2002.

Post-print version of the article: A. Steinboeck, D. Wild, T. Kiefer, and A. Kugi, "A mathematical model of a slab reheating furnace with radiative heat transfer and non-participating gaseous media", *International Journal of Heat and Mass Transfer*, vol. 53, no. 25-26, pp. 5933–5946, 2010. DOI: 10.1016/j.ijheatmasstransfer.2010.07.029
The content of this post-print version is identical to the published paper but without the publisher's final layout or copy editing.

[22] M.Y. Kim. A heat transfer model for the analysis of transient heating of the slab in a direct-fired walking beam type reheating furnace. *International Journal of Heat and Mass Transfer*, 50:3740–3748, 2007.

[23] H.S. Ko, J. Kim, T. Yoon, M. Lim, D.R. Yang, and I.S. Jun. Modeling and predictive control of a reheating furnace. *Proceedings of the American Control Conference, Chicago, USA*, 4:2725–2729, 2000.

[24] B. Leden. A control system for fuel optimization of reheating furnaces. *Scandinavian Journal of Metallurgy*, 15:16–24, 1986.

[25] Z. Li, P.V. Barr, and J.K. Brimacombe. Computer simulation of the slab reheating furnace. *Canadian Metallurgical Quarterly*, 27(3):187–196, 1988.

[26] P. Marino, A. Pignotti, and D. Solis. Numerical model of steel slab reheating in pusher furnaces. *Latin Amercian Applied Research*, 32(3):257–261, 2002.

[27] M.F. Modest. *Radiative Heat Transfer*. Academic Press, New York, 2nd edition, 2003.

[28] J.J. Noble. The zone method: Explicit matrix relations for total exchange areas. *International Journal for Heat and Mass Transfer*, 18:261–269, 1975.

[29] L.M. Pedersen and B. Wittenmark. On the reheat furnace control problem. *Proceedings of the American Control Conference*, pages 3811–3815, June 1998.

[30] B.D. Reddy. *Introductory Functional Analysis*. Texts in Applied Mathematics. Springer, New York, 1997.

[31] J.M. Rhine and R.J. Tucker. *Modelling of gas-fired furnaces and boilers and other industrial heating processes*. McGraw-Hill, London, UK, 1991.

[32] J.L. Roth, H. Sierpinski, J. Chabanier, and J.M. Germe. Computer control of slab furnaces based on physical models. *Iron and Steel Engineer*, 63(8):41–47, August 1986.

[33] Y. Samyudia and H. Sibarani. Identification of reheat furnace temperature models from closed-loop data—an industrial case study. *Asia-Pacific Journal of Chemical Engineering*, 1:70–81, 2006.

[34] R.J. Schurko, C. Weinstein, M.K. Hanne, and D.J. Pellecchia. Computer control of reheat furnaces: A comparison of strategies and applications. *Iron and Steel Engineer*, 64(5):37–42, May 1987.

[35] J.L.V.A. Sousa, J. Ward, R.A. Wallis, and D.A. Lawson. Simulation and measurement of the transient performance of a gas-fired heat treatment furnace. *Proceedings of the 2nd European Thermal-Sciences and 14th UIT National Heat Transfer Conference*, May 1996.

[36] D.F.J. Staalman and A. Kusters. On-line slab temperature calculation and control. *Manufacturing Science and Engineering*, 4:307–314, 1996.

[37] A. Steinboeck, D. Wild, T. Kiefer, and A. Kugi. A flexible time integration method for the 1D heat conduction problem. *Proceedings of the 6th Vienna Conference on Mathematical Modelling, Vienna, Austria, ARGESIM Report no. 35*, pages 1204–1214, February 2009.

[38] D.N. Trivic and C.H. Amon. Modeling the 3-D radiation of anisotropically scattering media by two different numerical methods. *International Journal of Heat and Mass Transfer*, 51:2711–2732, 2008.

[39] M. Vidyasagar. *Nonlinear systems analysis*. Number 42 in Classics in Applied Mathematics. SIAM, Philadelphia, USA, 2nd edition, 1992.

[40] D. Wild, T. Meurer, and A. Kugi. Modelling and experimental model validation for a pusher-type reheating furnace. *Mathematical and Computer Modelling of Dynamical Systems*, 15(3):209–232, June 2009.

[41] D. Wild, T. Meurer, A. Kugi, O. Fichet, and K. Eberwein. Nonlinear observer design for pusher-type reheating furnaces. *Proceedings of the 3rd International Steel Conference on New Developments in Metallurgical Process Technologies, Düsseldorf, Germany*, pages 790–797, June 2007.

[42] N. Yoshitani, T. Ueyama, and M. Usui. Optimal slab heating control with temperature trajectory optimization. *Proceedings of the 20th International Conference on Industrial Electronics, Control and Instrumentation, IECON'94*, 3:1567–1572,

Post-print version of the article: A. Steinboeck, D. Wild, T. Kiefer, and A. Kugi, "A mathematical model of a slab reheating furnace with radiative heat transfer and non-participating gaseous media", *International Journal of Heat and Mass Transfer*, vol. 53, no. 25-26, pp. 5933–5946, 2010. DOI: 10.1016/j.ijheatmasstransfer.2010.07.029
The content of this post-print version is identical to the published paper but without the publisher's final layout or copy editing.

September 1994.

[43] B. Zhang, Z. Chen, L. Xu, J. Wang, J. Zhang, and H. Shao. The modeling and control of a reheating furnace. *Proceedings of the American Control Conference, Anchorage, Alaska, USA*, pages 3823–3828, May 2002.

[44] O.C. Zienkiewicz and K. Morgan. *Finite elements and approximation.* Wiley, New York, May 1983.

Post-print version of the article: A. Steinboeck, D. Wild, T. Kiefer, and A. Kugi, "A mathematical model of a slab reheating furnace with radiative heat transfer and non-participating gaseous media", *International Journal of Heat and Mass Transfer*, vol. 53, no. 25-26, pp. 5933–5946, 2010. DOI: 10.1016/j.ijheatmasstransfer.2010.07.029
The content of this post-print version is identical to the published paper but without the publisher's final layout or copy editing.